THE
PHYSICAL
SOCIETY

MEMOIRS

OF THE

COLLEGE OF SCIENCE

UNIVERSITY OF KYOTO

SERIES A

VOL. XXVII, No. 1

April 1953

KYOTO

11273

MEMOIRS OF THE COLLEGE OF SCIENCE, University of Kyoto, Series A,
Vol. XXVII, No. 1, Article 1, 1953

A NOTE ON THE SKIN FRICTION OF A FLAT PLATE TO OSEEN'S APPROXIMATION

BY

S. TOMOTIKA

(Received August 1, 1952)

SUMMARY

A second approximation for the skin friction at small Reynolds numbers of a flat plate placed edgeways along a steady uniform stream was first obtained by Piercy and Winny as early as 1933, by pursuing Bairstow, Cave, and Lang's general analysis based upon Oseen's equations of motion. Their analysis is now extended to a third approximation and an expansion formula correct to the fourth power of the Reynolds number is derived for the skin friction of the flat plate. The formula is found to be in perfect agreement with that obtained recently by Aoi and the present writer by developing quite a different analysis on the basis of Oseen's equations of motion.

1. Introduction

The skin friction at small Reynolds numbers of a flat plate placed edgeways along a steady uniform stream has been calculated by some writers. In 1933 Piercy and Winny (**1**), pursuing Bairstow, Cave, and Lang's analysis (**2**) based upon Oseen's equations of motion, obtained a second approximation (to the order of R^2) for the skin friction coefficient of a flat plate, where R is the Reynolds number defined in terms of the uniform-stream velocity U and the length, d, of the plate as $R = Ud/\nu$. In 1941 Davies (**3**), pursuing Lewis's work (**4**), also calculated a similar second approximation for the skin friction of the plate, on the basis of the extended Oseen's equations of motion due originally to Southwell and Squire (**5**). Recently, Sidrak (**6**) has made a study, on the basis of Oseen's equations, on the steady flow of an incompressible viscous fluid past an elliptic cylinder whose major-axis is parallel to a uniform stream, and has calculated a second approximation for the drag coefficient of such an elliptic cylinder. Further, he has derived, as its limiting case, an expansion formula similar to those given by Piercy and Winny, and by Davies for the skin friction coefficient of the flat plate.

No complete agreement can be found among these three expansion formulae, however; they differ slightly from each other. Thus, if we denote the skin friction coefficient of the flat plate by C_D, the three formulae take the following forms:

Piercy and Winny:

$$C_D = \frac{4\pi}{R(1+S_1)}\left[1 - \frac{1}{1+S_1}\left(\frac{1}{2}S_1^2 + \frac{1}{2}S_1 - 0.2083\right)\left(\frac{R}{8}\right)^2\right];$$

Davies:

$$C_D = \frac{4\pi}{R(1+S_1)}\left[1 - \frac{1}{1+S_1}\left(\frac{1}{2}S_1^2 + S_1 - 0.2083\right)\left(\frac{R}{8}\right)^2\right];$$

Sidrak:

$$C_D = \frac{4\pi}{R(1+S_1)}\left[1 - \frac{1}{1+S_1}\left(\frac{1}{2}S_1^2 + \frac{1}{4}S_1 + 0.3364\right)\left(\frac{R}{8}\right)^2\right],$$

where we have put for convenience†

$$S_1 = -\gamma - \log\frac{1}{16}R,$$

$\gamma = 0.57721\cdots\cdots$ being Euler's constant.

Davies attributes the discrepancy between his own formula and Piercy and Winny's to the difference of Southwell and Squire's equations of motion, upon which his analysis is based, from those of Oseen. But, it is seen without difficulty that in a special case of the flat plate edgeways along the uniform stream, Southwell and Squire's equations are quite equivalent to Oseen's equations, and therefore it may be expected that the discrepancy between their formulae might be due to incompleteness of, or some errors in, either or both of their analyses.

Quite recently, Yosinobu and the present writer (**7**) have examined carefully Davies's analysis and it has been found that an expansion formula in perfect agreement with Piercy and Winny's can be derived for the skin friction coefficient of the flat plate by pursuing Davies's original work, if, in place of $\mathrm{Cek}_n(\xi)$ and $\mathrm{Sek}_n(\xi)$ used by himself, we use $\mathrm{Fek}_n(\xi)$ and $\mathrm{Gek}_n(\xi)$ for solutions of the modified Mathieu equation, which are expressed in more rapidly convergent series in products of the modified Bessel functions.

Further, a very careful examination on Sidrak's work has also been made by Yosinobu and the present writer (**8**) and it has been found that Sidrak makes several grave errors in the course of his analysis so that his results cannot be relied on. Developing correct analysis along the lines of Sidrak's work, we have shown that an expansion formula in complete agreement with Piercy and Winny's is again obtained.

On the other hand, Aoi and the present writer (**9**) have recently made, independently of Sidrak's work, a detailed study on the slow motion of a viscous liquid past an elliptic cylinder on the basis of Oseen's equations, and have obtained a general expression as well as an expansion formula correct to the fourth power of the Reynolds number for the drag of the elliptic cylinder. A third approximation for the skin friction coefficient of a flat plate has also been obtained as a limiting case of the expansion formula for the drag of the elliptic cylinder, and thus it has been found that up to the second approximation, our formula is in complete agreement with Piercy and Winny's.

Such a third approximation for the skin friction coefficient of the flat plate might have been alternatively obtained by extending Piercy and Winny's analysis, and this enquiry is the subject of the present note.

2. First and second approximations for the skin friction of the flat plate

Although both the first and second approximations for the skin friction of the flat plate have been obtained by Piercy and Winny (**1**), pursuing Bairstow, Cave, and Lang's general analysis, we shall first recapitulate their analysis for the sake of reference.

† This S_1 is equivalent to S in Sidrak's analysis. Strictly speaking, the figure 0.2083 should be replaced by 5/24.

We assume that the motion is two-dimensional and that a flat plate is placed edgeways along a steady uniform stream of velocity U of infinite extent. For convenience the length d of the plate is given the value 2, and ratio of U to ν, the kinematic coefficient of viscosity of the fluid, is denoted by $2k$. Then, the Reynolds number, R, as defined in terms of U and the length $d(=2)$ of the plate, becomes

$$R = Ud/\nu = 4k . \tag{2. 1}$$

Taking the origin at the nose of the plate and the x-axis along the plate in the downstream direction of the uniform stream, let us denote by E and M two points which may occupy any positions on the plate and write ξ_E, ξ_M for kx_E, kx_M respectively, and put $\xi_M - \xi_E = w$.

The equation obtained by Bairstow, Cave, and Lang (**2**, equation E (13)) for the distribution χ_E of doublets along the plate appropriate to the problem is

$$\frac{\pi U}{2} = \int_0^{2k} \left\{ e^w K_0(w) - \frac{1}{2}\frac{\partial}{\partial w}\left[e^w K_0(w) + \frac{1}{2}\log w^2 \right] \right\} \chi'(\xi_E)\, d\xi_E , \tag{2. 2}$$

where $\chi'(\xi_E) = \partial\chi_E/\partial\xi_E$ and K_0 is the modified Bessel function. These doublets satisfy the equation of viscous motion to Oseen's approximation, i. e.

$$\nu\nabla^4\psi = U\nabla^2(\partial\psi/\partial x) ,$$

and χ_E as obtained from (2. 2) satisfies the boundary conditions at the surface of the plate.

A solution for χ_E gives immediately the skin friction D of unit span of the plate by the relation (**2**, formula F (8)):

$$D = 4\mu \int_{x_E=0}^{x_E=2} d\chi_E , \tag{2. 3}$$

where $\mu = \rho\nu$ is the coefficient of viscosity of the fluid.

First approximation

With the origin changed to midway along the plate, equation (2. 2) may be written as:

$$\pi U = \int_{-k}^{k} \left\{ e^w \left[K_0(w) - \frac{\partial}{\partial w} K_0(w) \right] - \frac{1}{w} \right\} \chi'(\xi_E)\, d\xi_E . \tag{2. 4}$$

Assuming w small and expanding the kernel, we find, retaining only first terms of the expansions,

$$\pi U = \int_{-k}^{k} \left(1 - \gamma - \log\frac{w}{2} \right) \chi'(\xi_E)\, d\xi_E , \tag{2. 5}$$

where $\gamma = 0.57721\cdots$ is Euler's constant.

To solve this integral equation we assume

$$\chi'(\xi_E) = A/\sqrt{(k^2 - \xi_E^2)} . \tag{2. 6}$$

Then, on performing integration we find

$$U = A(1 + S_1), \tag{2.7}$$

where we have put for brevity

$$S_1 = -\gamma - \log\frac{1}{4}k = -\gamma - \log\frac{1}{16}R. \tag{2.8}$$

Hence (2.6) is a solution of (2.5) if

$$A = U/(1 + S_1). \tag{2.9}$$

In this case the distribution χ_E of doublets along the plate is given by

$$\chi_E = \int_{-k}^{\xi_E} \chi'(\xi_E)\,d\xi_E = \frac{U}{1 + S_1}\left(\frac{\pi}{2} + \sin^{-1}x_E\right), \tag{2.10}$$

and the expression for the skin friction D of the plate becomes

$$D = 4\mu(\chi_1 - \chi_{-1}) = 4\mu\pi U/(1 + S_1). \tag{2.11}$$

If, as usual, we define the skin friction coefficient C_D by

$$C_D = D/(\rho U^2 d),$$

we obtain

$$C_D = \frac{1}{k}\frac{\chi_1 - \chi_{-1}}{U} = \frac{4\pi}{R(1 + S_1)}. \tag{2.12}$$

This is the first approximation for the skin friction coefficient of the flat plate.

Second approximation

Next, expanding the kernel of (2.4) as before, but retaining squares of small quantities, the integral equation for determining the distribution χ_E of doublets becomes

$$\pi U = \int_{-k}^{k}\left\{-\left(\gamma + \log\frac{1}{2}w\right)\left(1 + \frac{1}{2}w + \frac{1}{4}w^2\right) + \left(1 + \frac{1}{4}w + \frac{1}{6}w^2\right)\right\}\chi'(\xi_E)\,d\xi_E. \tag{2.13}$$

It is now assumed for the form of the solution that

$$\chi'(\xi_E) = \frac{A + B\xi_E + C\xi_E^2}{\sqrt{(k^2 - \xi_E^2)}}. \tag{2.14}$$

After substitution and reduction, we first obtain, by equating the coefficients of ξ_M,

$$\left(\frac{1}{4} - \frac{1}{2}S_1\right)A = \left\{1 + \left(\frac{1}{12} - \frac{1}{4}S_1\right)k^2\right\}B - \left(\frac{1}{4} - \frac{1}{4}S_1\right)k^2C, \tag{2.15}$$

and next, by equating those of ξ_M^2,

$$\left(\frac{5}{12} - \frac{1}{2}S_1\right)A = \frac{1}{2}B + \left\{1 - \left(\frac{1}{3} - \frac{1}{4}S_1\right)k^2\right\}C. \tag{2.16}$$

Solving B and C from these two equations we find

$$\left.\begin{aligned}\frac{B}{A} &= \frac{1}{4} - \frac{1}{2}S_1 + O(k^2)\,,\\ \frac{C}{A} &= \frac{7}{24} - \frac{1}{4}S_1 + O(k^2)\,.\end{aligned}\right\} \tag{2.17}$$

On the other hand, on equating constant terms and taking account of (2.17), we have, to the order of k^2,

$$\frac{U}{A} = 1 + S_1 + \frac{1}{8}\left(\frac{3}{4} + \frac{7}{6}S_1\right)k^2\,. \tag{2.18}$$

These values of A, B, C make (2.14) to satisfy the integral equation (2.13) to the order of k^2, and to the same order the distribution χ_E of doublets along the plate is found to be given by

$$\chi_E = A\left(\frac{\pi}{2} + \sin^{-1}x_E\right) - Bk\sqrt{(1 - x_E^2)} + \frac{1}{2}Ck^2\left\{\frac{\pi}{2} + \sin^{-1}x_E - x_E\sqrt{(1 - x_E^2)}\right\}. \tag{2.19}$$

The skin friction D of the plate now becomes

$$D = 4\mu(\chi_1 - \chi_{-1}) = 4\mu\pi\left(A + \frac{1}{2}Ck^2\right), \tag{2.20}$$

and calculating the skin friction coefficient C_D as in the preceding case of the first approximation, we get finally

$$C_D = \frac{\pi}{k}\,\frac{1 + \frac{1}{8}\left(\frac{7}{6} - S_1\right)k^2}{1 + S_1 + \frac{1}{8}\left(\frac{3}{4} + \frac{7}{6}S_1\right)k^2}\,. \tag{2.21}$$

This result is due originally to Piercy and Winny.

Correct to the order of $k^2\left(=\frac{1}{16}R^2\right)$, the above formula may also be written in the form:

$$C_D = \frac{4\pi}{R(1 + S_1)}\left\{1 - \frac{1}{1 + S_1}\left(\frac{1}{2}S_1^2 + \frac{1}{2}S_1 - \frac{5}{24}\right)\left(\frac{R}{8}\right)^2\right\}, \tag{2.22}$$

which has been quoted by Sidrak (**6**) as Piercy and Winny's second approximate formula.

If, in place of S_1, we use S such that

$$S = 1 + S_1 = 1 - \gamma - \log\frac{1}{16}R\,, \tag{2.23}$$

the two formulae (2.12) and (2.22) become respectively

$$C_D = \frac{4\pi}{RS}\,, \tag{2.24}$$

$$C_D = \frac{4\pi}{RS}\left\{1 - \frac{1}{S}\left(S^2 - S - \frac{5}{12}\right)\frac{R^2}{128}\right\}. \tag{2.25}$$

3. A third approximation for the skin friction of the flat plate

In order to extend the preceding analysis to a third approximation, we must retain terms up to the order of w^4 in the expansion of the kernel in (2.4). Then, the integral equation for determining the distribution χ_E of doublets along the plate becomes

$$\pi U = \int_{-k}^{k} \left\{ -\left(\gamma + \log\frac{1}{2}w\right)\left(1 + \frac{1}{2}w + \frac{1}{4}w^2 + \frac{5}{48}w^3 + \frac{7}{192}w^4\right) + \left(1 + \frac{1}{4}w + \frac{1}{6}w^2 + \frac{17}{192}w^3 + \frac{71}{1920}w^4\right)\right\} \chi'(\xi_E)\, d\xi_E . \tag{3.1}$$

For the form of the solution we assume

$$\chi'(\xi_E) = \frac{A + B\xi_E + C\xi_E^2 + D\xi_E^3 + E\xi_E^4}{\sqrt{(k^2 - \xi_E^2)}} . \tag{3.2}$$

After substitution and reduction, we find, correct to the order of k^4, that

on equating constant terms,

$$U = \left\{1 + S_1 + \left(\frac{1}{48} + \frac{1}{8}S_1\right)k^2 + \left(\frac{181}{30720} + \frac{7}{512}S_1\right)k^4\right\} A - \left\{\frac{1}{4}S_1 k^2 + \left(\frac{1}{96} + \frac{5}{128}S_1\right)k^4\right\} B + \left\{\left(\frac{1}{4} + \frac{1}{2}S_1\right)k^2 + \left(\frac{1}{128} + \frac{3}{32}S_1\right)k^4\right\} C + \left(\frac{1}{64} - \frac{3}{16}S_1\right)k^4 D + \left(\frac{5}{32} + \frac{3}{8}S_1\right)k^4 E ; \tag{3.3}$$

on equating the coefficients of ξ_M,

$$\left\{-\left(\frac{1}{4} - \frac{1}{2}S_1\right) + \left(\frac{1}{384} + \frac{5}{32}S_1\right)k^2\right\} A + \left\{1 + \left(\frac{1}{12} - \frac{1}{4}S_1\right)k^2 - \left(\frac{19}{1920} + \frac{7}{128}S_1\right)k^4\right\} B - \left\{\left(\frac{1}{4} - \frac{1}{4}S_1\right)k^2 + \left(\frac{1}{128} - \frac{15}{128}S_1\right)k^4\right\} C + \left\{\frac{1}{2}k^2 + \left(\frac{5}{64} - \frac{3}{16}S_1\right)k^4\right\} D - \left(\frac{13}{64} - \frac{3}{16}S_1\right)k^4 E = 0 ; \tag{3.4}$$

on equating the coefficients of ξ_M^2,

$$-\left\{\left(\frac{5}{24}-\frac{1}{4}S_1\right)+\left(\frac{29}{3840}-\frac{7}{64}S_1\right)k^2\right\}A$$

$$+\left\{\frac{1}{4}+\left(\frac{29}{384}-\frac{5}{32}S_1\right)k^4\right\}B$$

$$+\left\{\frac{1}{2}-\left(\frac{1}{6}-\frac{1}{8}S_1\right)k^2-\left(\frac{1}{80}-\frac{21}{256}S_1\right)k^4\right\}C$$

$$+\left\{\frac{1}{8}k^2+\left(\frac{17}{256}-\frac{15}{128}S_1\right)k^4\right\}D$$

$$+\left\{\frac{1}{4}k^2-\left(\frac{17}{128}-\frac{3}{32}S_1\right)k^4\right\}E=0\,; \tag{3.5}$$

on equating the coefficients of ξ_M^3,

$$-\left(\frac{59}{576}-\frac{5}{48}S_1\right)A$$

$$+\left\{\frac{1}{12}+\left(\frac{239}{5760}-\frac{7}{96}S_1\right)k^2\right\}B$$

$$+\left\{\frac{1}{12}-\left(\frac{89}{1152}-\frac{5}{96}S_1\right)k^2\right\}C$$

$$+\left\{\frac{1}{3}+\frac{1}{24}k^2+\left(\frac{137}{3840}-\frac{7}{128}S_1\right)k^4\right\}D$$

$$+\left\{\frac{1}{24}k^2-\left(\frac{47}{768}-\frac{5}{128}S_1\right)k^4\right\}E=0\,; \tag{3.6}$$

and finally on equating the coefficients of ξ_M^4,

$$-\left(\frac{449}{11520}-\frac{7}{192}S_1\right)A+\frac{5}{192}B$$

$$+\left\{\frac{1}{48}-\left(\frac{659}{23040}-\frac{7}{384}S_1\right)k^2\right\}C$$

$$+\left(\frac{1}{24}+\frac{5}{384}k^2\right)D$$

$$+\left\{\frac{1}{4}+\frac{1}{96}k^2-\left(\frac{347}{15360}-\frac{7}{512}S_1\right)k^4\right\}E=0\,. \tag{3.7}$$

Solving the four equations (3.4), (3.5), (3.6), and (3.7) we obtain

$$\left.\begin{aligned}
\frac{B}{A} &= \frac{1}{4} - \frac{1}{2}S_1 - \left(\frac{7}{192} + \frac{1}{8}S_1 + \frac{1}{16}S_1^2\right)k^2 + O(k^4), \\
\frac{C}{A} &= \frac{7}{24} - \frac{1}{4}S_1 + \left(\frac{131}{11520} - \frac{13}{128}S_1 - \frac{1}{16}S_1^2\right)k^2 + O(k^4), \\
\frac{D}{A} &= \frac{11}{64} - \frac{1}{8}S_1 + O(k^2), \\
\frac{E}{A} &= \frac{443}{5760} - \frac{5}{96}S_1 + O(k^2).
\end{aligned}\right\} \tag{3.8}$$

Substituting these values in (3.3), we obtain, after some reductions,

$$\frac{U}{A} = 1 + S_1 + \frac{1}{8}\left(\frac{3}{4} + \frac{7}{6}S_1\right)k^2 + \frac{1}{64}\left(\frac{213}{144} + \frac{481}{720}S_1 - \frac{9}{4}S_1^2 - S_1^3\right)k^4. \tag{3.9}$$

These values of A, B, C, D, E make (3.2) to satisfy the integral equation (3.1) to the order of k^4, and to the same order the distribution χ_E of doublets along the plate is obtained as:

$$\begin{aligned}
\chi_E = {} & A\left(\frac{\pi}{2} + \sin^{-1}x_E\right) - Bk\sqrt{(1 - x_E^2)} \\
& + \frac{1}{2}Ck^2\left\{\frac{\pi}{2} + \sin^{-1}x_E - x_E\sqrt{(1 - x_E^2)}\right\} \\
& - \frac{1}{3}Dk^3\left\{2\sqrt{(1 - x_E^2)} + x_E^2\sqrt{(1 - x_E^2)}\right\} \\
& + Ek^4\left\{\frac{3\pi}{16} + \frac{3}{8}\sin^{-1}x_E - \frac{3}{8}x_E\sqrt{(1 - x_E^2)} - \frac{1}{4}x_E^3\sqrt{(1 - x_E^2)}\right\}.
\end{aligned} \tag{3.10}$$

The skin friction coefficient C_D of the plate now becomes

$$C_D = \frac{\pi A}{kU}\left(1 + \frac{1}{2}\frac{C}{A}k^2 + \frac{3}{8}\frac{E}{A}k^4\right), \tag{3.11}$$

and if we substitute the values of C/A, E/A and U/A as given by (3.8) and (3.9), we ultimately obtain a third approximation for C_D in the form:

$$\begin{aligned}
C_D = {} & \frac{4\pi}{R(1 + S_1)}\left\{1 - \frac{1}{1 + S_1}\left(S_1^2 + S_1 - \frac{5}{12}\right)\frac{R^2}{128}\right. \\
& \left. - \frac{1}{(1 + S_1)^2}\left(S_1^4 + \frac{49}{12}S_1^3 + \frac{381}{72}S_1^2 + \frac{707}{360}S_1 - \frac{301}{720}\right)\frac{R^4}{128^2}\right\}.
\end{aligned} \tag{3.12}$$

If, as before, use is made of $S(= 1 + S_1)$ in place of S_1, the formula may be put in the form:

$$C_D = \frac{4\pi}{RS}\left\{1 - \frac{1}{S}\left(S^2 - S - \frac{5}{12}\right)\frac{R^2}{128}\right.$$

$$\left. - \frac{1}{S^2}\left(S^4 + \frac{1}{12}S^3 - \frac{23}{24}S^2 - \frac{133}{360}S - \frac{25}{144}\right)\frac{R^4}{128^2}\right\}. \quad (3.13)$$

This is in complete agreement with the formula obtained recently by Aoi and the present writer (**9**) by developing quite a different analysis.

REFERENCES

1. N. A. V. Piercy and H. F. Winny, 'The skin friction of flat plates to Oseen's approximation', *Proc. Roy. Soc.* A, **140** (1933), 543.
2. L. Bairstow, B. M. Cave, and E. D. Lang, 'The resistance of a cylinder moving in a viscous fluid', *Phil. Trans. Roy. Soc.* A, **223** (1923), 383.
3. T. V. Davies, 'An investigation of the flow of a viscous fluid past a flat plate, using elliptic coordinates', *Phil. Mag.*, **31** (1941), 283.
4. T. Lewis, 'Solutions of Oseen's extended equations for circular and elliptic cylinders and a flat plate', *Quart. Journ. Math.*, Oxford Series, **9** (1938), 21.
5. R. V. Southwell and H. B. Squire, 'A modification of Oseen's approximate equation for the motion in two dimensions of a viscous incompressible fluid', *Phil. Trans. Roy. Soc.* A, **232** (1933), 27.
6. S. Sidrak, 'The flow of a viscous liquid past an elliptic cylinder', *Proc. Roy. Irish Acad.*, **53** (1950), 65.
7. S. Tomotika and H. Yosinobu, 'The flow of a viscous liquid past a flat plate at small Reynolds numbers'. (To be published shortly)
8. S. Tomotika and H. Yosinobu, 'The drag on an elliptic cylinder moving in a viscous liquid at small Reynolds numbers', *Memoirs Coll. Sci., Univ. of Kyoto*, A **27** (1953), 11.
9. S. Tomotika and T. Aoi, 'The steady flow of a viscous fluid past an elliptic cylinder and a flat plate at small Reynolds numbers'. To appear soon in *Quart. Journ. Mech. and Applied Math.*

Memoirs of the College of Science, University of Kyoto, Series A,
Vol. XXVII, No. 1, Article 2, 1953

THE DRAG ON AN ELLIPTIC CYLINDER MOVING IN A VISCOUS LIQUID AT SMALL REYNOLDS NUMBERS

BY

S. TOMOTIKA AND H. YOSINOBU

(*Received October 15, 1952*)

SUMMARY

Pursuing Sidrak's lines of attack, the steady flow of an incompressible viscous fluid past an elliptic cylinder has been discussed, on the basis of Oseen's linearized equations of motion, in case when the major-axis of the ellipse is parallel to the undisturbed uniform stream. The exact solution of Oseen's equations has been first obtained and then the general expression for the drag experienced by the elliptic cylinder has been calculated. Also, an expansion formula correct to the second power of Reynolds number has been derived for the drag coefficient of the cylinder. The expansion formula thus derived is in complete agreement, to the second approximation, with a similar expansion formula which has been obtained recently by Tomotika and Aoi.

1. Introduction

The steady flow of an incompressible viscous fluid past an elliptic cylinder at small Reynolds numbers was studied so far by several writers. In 1924 Harrison (**1**), solving Oseen's equations of motion approximately, calculated a first approximation for the drag per unit span of an elliptic cylinder whose major-axis is parallel to a steady uniform flow. In 1937 Meksyn (**2**) discussed, on the basis of the same Oseen's equations, the flow past an elliptic cylinder set obliquely at an arbitrary angle of incidence in a uniform flow and computed, though only numerically, the drag and lift of the cylinder. In the next year 1938 Lewis (**3**) treated the flow of an incompressible viscous fluid past circular and elliptic cylinders and a flat plate, by using Oseen's extended equations of motion due originally to Southwell and Squire. After pointing out that in Meksyn's solution the circulation round the obstacle is infinite, Lewis obtained an improved solution which gives rise to finite circulation. However, no discussions have been made on the drag and lift of the elliptic cylinder. Further, Sidrak (**4**) has lately discussed the flow of a viscous liquid past an elliptic cylinder, on the basis of Oseen's equations, with the intention of obtaining approximate expansion formulae in powers of Reynolds number for the drag of an elliptic cylinder as well as of a flat plate, each placed parallel to the uniform stream. On examining his paper carefully it has been found, however, that he makes several grave errors in the course of his analysis so that his results are not reliable.

In a quite recent paper (**5**), Aoi and one of the present writers (S. T.) have also made, independently of Sidrak, detailed theoretical discussions based upon Oseen's equations of motion on the steady flow of a viscous liquid around an elliptic cylinder or a flat plate placed parallel or perpendicularly to a uniform stream, and the drag experienced by, and the flow patterns around, the obstacle have been discussed in detail by making

use of the exact solution of Oseen's equations. Also, approximate expansion formulae for the drag have been obtained in each case correct to the fourth power of the Reynolds number.

Such expansion formulae should have been obtained as well by pursuing Sidrak's lines of attack, if correct analysis would have been developed; and to the discussion of the matter the present paper is directed.

2. The general solution of Oseen's equations of motion

We consider an infinitely long elliptic cylinder, with major-and minor-axes of length $2a$ and $2b$ respectively, set at right angles to a steady uniform stream of velocity U of an incompressible viscous fluid in such a manner that its major-axis is parallel to the uniform stream. Let (x, y) be the rectangular coordinates having the origin at the centre of the ellipse and the axes of x and y along the major- and minor-axes respectively. We denote by $U+u, v$ the components of the fluid velocity at any point, so that u, v are the velocity of perturbation which become vanishingly small everywhere at a great distance from the cylinder. If squares of u, v are omitted, we get, from the Navier-Stokes equations of motion, the well-known linearized equation of Oseen:

$$U\frac{\partial}{\partial x}(u,\ v) = -\frac{1}{\rho}\left(\frac{\partial}{\partial x},\ \frac{\partial}{\partial y}\right)p + \nu\nabla^2(u,\ v)\,, \tag{2.1}$$

where p is the pressure, ρ the density of the fluid, ν its kinematic coefficient of viscosity, and ∇^2 stands for $\partial^2/\partial x^2+\partial^2/\partial y^2$. The fluid being assumed to be incompressible, the equation of continuity is

$$\frac{\partial u}{\partial x} + \frac{\partial v}{\partial y} = 0\,. \tag{2.2}$$

If we put $k=U/2\nu$, these equations are satisfied by

$$\left.\begin{aligned} u &= -\frac{\partial\phi}{\partial x} + \frac{1}{2k}\frac{\partial\chi}{\partial x} - \chi\,,\\ v &= -\frac{\partial\phi}{\partial y} + \frac{1}{2k}\frac{\partial\chi}{\partial y}\,, \end{aligned}\right\} \tag{2.3}$$

and

$$p = \rho U\frac{\partial\phi}{\partial x}\,, \tag{2.4}$$

provided that

$$\nabla^2\phi = 0\,, \tag{2.5}$$

and

$$\nabla^2\chi - 2k\frac{\partial\chi}{\partial x} = 0\,. \tag{2.6}$$

We now introduce the elliptic coordinates (ξ, η) defined as:

$$x + iy = c\cosh(\xi + i\eta)\,,$$

with $c=\sqrt{a^2-b^2}$.

Then, equation (2.5) becomes

$$\frac{\partial^2\phi}{\partial\xi^2}+\frac{\partial^2\phi}{\partial\eta^2}=0\,, \tag{2.7}$$

and, if we put $\chi=e^{kx}\chi_1$ in (2.6), the equation for χ_1 becomes

$$\frac{\partial^2\chi_1}{\partial\xi^2}+\frac{\partial^2\chi_1}{\partial\eta^2}-k^2c^2(\cosh^2\xi-\cos^2\eta)\chi_1=0\,. \tag{2.8}$$

Bearing in mind that the flow past the cylinder is symmetrical about the axis of x and that the perturbation due to the presence of the body must vanish at infinity, the appropriate general solution of equation (2.7) is given by

$$\phi=cUb_0\xi-cU\sum_{n=1}^{\infty}\frac{1}{n}b_ne^{-n\xi}\cos n\eta\,, \tag{2.9}$$

where the b_n's are constants of integration.

Next, in order to solve equation (2.8) we put $\chi_1=F(\xi)G(\eta)$ and separate the variables. Then we are led to the modified Mathieu equation for $F(\xi)$ and the Mathieu equation for $G(\eta)$, namely:

$$\frac{d^2F}{d\xi^2}-(\lambda+k^2c^2\cosh^2\xi)F=0\,, \tag{2.10}$$

$$\frac{d^2G}{d\eta^2}+(\lambda+k^2c^2\cos^2\eta)G=0\,. \tag{2.11}$$

Solutions, periodic in η with period 2π, of equation (2.11) are obtained for a discrete set of characteristic values of λ. They fall into the four groups:

$$\left.\begin{aligned}
\mathrm{ce}_{2n}(\eta)&=\sum_{r=0}^{\infty}a_{2r}^{(2n)}\cos 2r\eta\,,\\
\mathrm{ce}_{2n+1}(\eta)&=\sum_{r=0}^{\infty}a_{2r+1}^{(2n+1)}\cos(2r+1)\eta\,,\\
\mathrm{se}_{2n+1}(\eta)&=\sum_{r=0}^{\infty}b_{2r+1}^{(2n+1)}\sin(2r+1)\eta\,,\\
\mathrm{se}_{2n+2}(\eta)&=\sum_{r=0}^{\infty}b_{2r+2}^{(2n+2)}\sin(2r+2)\eta\,.
\end{aligned}\right\} \tag{2.12}$$

The corresponding pairs of solutions of equation (2.10) which tend to zero when $\xi\to\infty$, are

$$\left.\begin{aligned}
\mathrm{Fek}_{2n}(\xi)&=\frac{p'_{2n}}{\pi a_0^{(2n)}}\sum_{r=0}^{\infty}(-1)^r a_{2r}^{(2n)}I_r(v_1)K_r(v_2)\,,\\
\mathrm{Fek}_{2n+1}(\xi)&=\frac{s'_{2n+1}}{\pi a_1^{(2n+1)}}\sum_{r=0}^{\infty}(-1)^r a_{2r+1}^{(2n+1)}[I_r(v_1)K_{r+1}(v_2)-I_{r+1}(v_1)K_r(v_2)]\,,
\end{aligned}\right\}$$

$$\left.\begin{aligned}\mathrm{Gek}_{2n+1}(\xi) &= \frac{p'_{2n+1}}{\pi b_1^{(2n+1)}}\sum_{r=0}^{\infty}(-1)^r b_{2r+1}^{(2n+1)}[I_r(v_1)K_{r+1}(v_2)+I_{r+1}(v_1)K_r(v_2)],\\ \mathrm{Gek}_{2n+2}(\xi) &= \frac{s'_{2n+2}}{\pi b_2^{(2n+2)}}\sum_{r=0}^{\infty}(-1)^r b_{2r+2}^{(2n+2)}[I_r(v_1)K_{r+2}(v_2)-I_{r+2}(v_1)K_r(v_2)],\end{aligned}\right\} \tag{2.13}$$

where $v_1=\frac{1}{2}kce^{-\xi}$, $v_2=\frac{1}{2}kce^{\xi}$ and p'_{2n}, p'_{2n+1}, s'_{2n+1}, s'_{2n+2} are all constants independent of ξ.

Since, in the present case, the flow is symmetrical about the axis of x, χ must be an even function with respect to η. Therefore, the appropriate general solution for χ is given by

$$\chi = Ue^{kc\cosh\xi\cos\eta}\sum_{m=0}^{\infty}a_m\mathrm{FEK}_m(\xi)\mathrm{ce}_m(\eta), \tag{2.14}$$

where the a_m's are constants of integration, and

$$\left.\begin{aligned}\mathrm{FEK}_{2n}(\xi) &= \frac{\pi}{p'_{2n}}\mathrm{Fek}_{2n}(\xi),\\ \mathrm{FEK}_{2n+1}(\xi) &= \frac{\pi}{s'_{2n+1}}\mathrm{Fek}_{2n+1}(\xi).\end{aligned}\right\} \tag{2.15}$$

Inserting the above general expressions for ϕ and χ into (2.3) and (2.4) we can readily obtain the expressions for the components u, v of the velocity of perturbation and the pressure p at any point. Thus we have

$$\begin{aligned}u = {}& \frac{U}{2h^2}\left[b_0e^{-\xi}\cos\eta + b_1e^{-2\xi} - \sum_{n=1}^{\infty}\{b_{n-1}e^{-(n-2)\xi} - b_{n+1}e^{-(n+2)\xi}\}\cos n\eta\right]\\ &+ \frac{U}{2kch^2}e^{kc\cosh\xi\cos\eta}\sum_{m=0}^{\infty}a_m\Big[\mathrm{FEK}_m'(\xi)\sinh\xi\,\mathrm{ce}_m(\eta)\cos\eta\\ &\qquad - \mathrm{FEK}_m(\xi)\Big\{\cosh\xi\,\mathrm{ce}_m'(\eta)\sin\eta + \frac{1}{2}kc\,\mathrm{ce}_m(\eta)(\cosh 2\xi - \cos 2\eta)\Big\}\Big],\end{aligned} \tag{2.16}$$

$$\begin{aligned}v = {}& -\frac{U}{2h^2}\left[b_0e^{-\xi}\sin\eta + \sum_{n=1}^{\infty}\{b_{n-1}e^{-(n-2)\xi} - b_{n+1}e^{-(n+2)\xi}\}\sin n\eta\right]\\ &+ \frac{U}{2kch^2}e^{kc\cosh\xi\cos\eta}\sum_{m=0}^{\infty}a_m\Big[\mathrm{FEK}_m'(\xi)\cosh\xi\,\mathrm{ce}_m(\eta)\sin\eta\\ &\qquad + \mathrm{FEK}_m(\xi)\sinh\xi\,\mathrm{ce}_m'(\eta)\cos\eta\Big],\end{aligned} \tag{2.17}$$

$$p = \frac{\rho U^2}{2h^2}\left[-(b_0e^{-\xi}\cos\eta + b_1e^{-2\xi}) + \sum_{n=1}^{\infty}\{b_{n-1}e^{-(n-2)\xi} - b_{n+1}e^{-(n+2)\xi}\}\cos n\eta\right], \tag{2.18}$$

where $\mathrm{FEK}_m'(\xi)=\frac{d}{d\xi}\mathrm{FEK}_m(\xi)$, $\mathrm{ce}_m'(\eta)=\frac{d}{d\eta}\mathrm{ce}_m(\eta)$ and $h^2=\frac{1}{2}(\cosh 2\xi-\cos 2\eta)$.

3. The boundary conditions

We shall now proceed to determine the constants of integration a_m's and b_n's by the boundary conditions. Since, however, the conditions at infinity are satisfied automatically by the preceding expressions (2.16) and (2.17) for the components of the velocity of perturbation, we have only to consider the conditions at the surface of the elliptic cylinder.

Assuming that the elliptic cylinder under consideration is defined by $\xi=\xi_0$, the said conditions become

$$u = -U, \quad v = 0 \tag{3.1}$$

at $\xi=\xi_0$.

Making use of the Fourier expansions:

$$e^{kc\cosh\xi\cos\eta}\Big[\mathrm{FEK}_m'(\xi)\sinh\xi\,\mathrm{ce}_m(\eta)\cos\eta - \mathrm{FEK}_m(\xi)\Big\{\cosh\xi\,\mathrm{ce}_m'(\eta)\sin\eta + \frac{1}{2}kc\,\mathrm{ce}_m(\eta)(\cosh 2\xi - \cos 2\eta)\Big\}\Big] = \sum_{n=0}^{\infty} G_{m,n}(\xi)\cos n\eta\,,$$

$$e^{kc\cosh\xi\cos\eta}\Big[\mathrm{FEK}_m'(\xi)\cosh\xi\,\mathrm{ce}_m(\eta)\sin\eta + \mathrm{FEK}_m(\xi)\sinh\xi\,\mathrm{ce}_m'(\eta)\cos\eta\Big] = \sum_{n=1}^{\infty} H_{m,n}(\xi)\sin n\eta\,,$$

the expressions (2.16) and (2.17) for u and v can be rewritten as:

$$h^2u = \frac{U}{2}\Big[b_0e^{-\xi}\cos\eta + b_1e^{-2\xi} - \sum_{n=1}^{\infty}\{b_{n-1}e^{-(n-2)\xi} - b_{n+1}e^{-(n+2)\xi}\}\cos n\eta\Big] + \frac{U}{2kc}\sum_{m=0}^{\infty}\sum_{n=0}^{\infty} a_mG_{m,n}(\xi)\cos n\eta\,, \tag{3.2}$$

and

$$h^2v = -\frac{U}{2}\Big[b_0e^{-\xi}\sin\eta + \sum_{n=1}^{\infty}\{b_{n-1}e^{-(n-2)\xi} - b_{n+1}e^{-(n+2)\xi}\}\sin n\eta\Big] + \frac{U}{2kc}\sum_{m=0}^{\infty}\sum_{n=0}^{\infty} a_mH_{m,n}(\xi)\sin n\eta\,. \tag{3.3}$$

Thus, substituting these expressions into the boundary conditions (3.1) and equating the coefficients of $\cos n\eta$ and $\sin n\eta$ ($n=0, 1, 2, \ldots$) on both sides of the equations, we get

$$b_1e^{-2\xi_0} + \frac{1}{kc}\sum_{m=0}^{\infty} a_mG_{m,0}(\xi) = -\cosh 2\xi_0\,, \tag{3.4}$$

$$\Big(b_0\sinh\xi_0 - \frac{1}{2}b_2e^{-\xi_0}\Big) - \frac{1}{2kc}\sum_{m=0}^{\infty} a_mG_{m,1}(\xi_0) = 0\,, \tag{3.5}$$

$$(b_1 - b_3 e^{-4\xi_0}) - \frac{1}{kc}\sum_{m=0}^{\infty} a_m G_{m,2}(\xi_0) = -1\,, \tag{3.6}$$

$$(b_{n-1}e^{-(n-2)\xi_0} - b_{n+1}e^{-(n+2)\xi_0}) - \frac{1}{kc}\sum_{m=0}^{\infty} a_m G_{m,n}(\xi_0) = 0\,; \tag{3.7}$$

$$(n = 3,\ 4,\ 5,\cdots)$$

$$\left(b_0 \cosh\xi_0 - \frac{1}{2}b_2 e^{-2\xi_0}\right) - \frac{1}{2kc}\sum_{m=0}^{\infty} a_m H_{m,1}(\xi_0) = 0\,, \tag{3.8}$$

$$(b_1 - b_3 e^{-4\xi_0}) - \frac{1}{kc}\sum_{m=0}^{\infty} a_m H_{m,2}(\xi_0) = 0\,, \tag{3.9}$$

$$(b_{n-1}e^{-(n-2)\xi_0} - b_{n+1}e^{-(n+2)\xi_0}) - \frac{1}{kc}\sum_{m=0}^{\infty} a_m H_{m,n}(\xi_0) = 0\,. \tag{3.10}$$

$$(n = 3,\ 4,\ 5,\cdots)$$

Subtracting (3.6) from (3.9) and (3.7) from (3.10), we obtain

$$\sum_{m=0}^{\infty} \lambda_{m,n} a_m = \begin{cases} kc\,, & (n = 2) \\ 0\,, & (n = 3,\ 4,\ 5,\cdots) \end{cases} \tag{3.11}$$

where

$$\lambda_{m,n} = G_{m,n}(\xi_0) - H_{m,n}(\xi_0)\,, \quad \begin{pmatrix} m = 0,\ 1,\ 2,\cdots \\ n = 1,\ 2,\ 3,\cdots \end{pmatrix} \tag{3.12}$$

and the a_m's can be determined by solving this system of simultaneous linear algebraic equations.

If use is made of the a_m's thus determined, the value of b_0 can be found by the following equation as given by eliminating b_2 between (3.5) and (3.8):

$$b_0 = -\frac{e^{\xi_0}}{2kc}\sum_{m=0}^{\infty} \lambda_{m,1} a_m\,, \tag{3.13}$$

and also the value of b_1 can be obtained by (3.4). The remaining b_n's can be determined successively from either of (3.7) and (3.10).

4. Transformation of the expressions for $\lambda_{m,n}$

Before proceeding to the calculation of the drag experienced by the elliptic cylinder under consideration, we shall now transform the expressions (3.12) for the $\lambda_{m,n}$'s into more convenient forms. To do this, we introduce functions $p_{m,n}(t)$ defined as:

$$p_{m,n}(t) = \frac{1}{\pi}\int_{-\pi}^{\pi} e^{t\cos\eta}\,\mathrm{ce}_m(\eta)\cos n\eta\, d\eta\,. \tag{4.1}$$

$$(m,\ n = 0,\ 1,\ 2,\cdots)$$

Substituting the series for $\mathrm{ce}_m(\gamma)$ as given by (2. 12) in the right-hand side and carrying out integrations, it is readily found that these functions $p_{m,n}(t)$ can be expressed as series of the modified Bessel functions*. Thus, we have

$$\left.\begin{aligned} p_{2m,n}(t) &= \sum_{r=0}^{\infty} a_{2r}^{(2m)}\{I_{n-2r}(t) + I_{n+2r}(t)\}, \\ p_{2m+1,n}(t) &= \sum_{r=0}^{\infty} a_{2r+1}^{(2m+1)}\{I_{n-2r-1}(t) + I_{n+2r+1}(t)\}. \end{aligned}\right\} \tag{4. 2}$$

In what follows we take

$$t = kc\cosh\xi_0 = ka, \tag{4. 3}$$

where $a=c\cosh\xi_0$ is the half-length of the major-axis of the ellipse $\xi=\xi_0$.

Then, writing for convenience's sake

$$\frac{1}{2}kc = q, \quad e^{\xi_0} = \sigma, \quad e^{-\xi_0} = \tau, \quad \omega = \sigma + \tau, \tag{4. 4}$$

and bearing in mind that

$$\sigma\tau = 1, \quad t = \omega q, \tag{4. 5}$$

the expressions (3. 12) for the $\lambda_{m,n}$'s can be transformed, after some calculations, into the following forms:

$$\lambda_{m,n} = \mathrm{FEK}_m'(\xi_0)\Phi_{m,n} - \mathrm{FEK}_m(\xi_0)\Psi_{m,n}, \tag{4. 6}$$
$$(m = 0, 1, 2, \cdots; \ n = 1, 2, 3, \cdots)$$

where

$$\left.\begin{aligned} \Phi_{m,n} &= \frac{1}{2}\left\{\sigma p_{m,n+1}(\omega q) - \tau p_{m,n-1}(\omega q)\right\}, \\ \Psi_{m,n} &= -\frac{1}{4}\left\{(\sigma^2 + 3)q p_{m,n+2}(\omega q) + 2(n+1)\sigma p_{m,n+1}(\omega q)\right. \\ &\quad - (3\sigma^2 + 2 + 3\tau^2)q p_{m,n}(\omega q) - 2(n-1)\tau p_{m,n-1}(\omega q) \\ &\quad \left. + (3 + \tau^2)q p_{m,n-2}(\omega q)\right\}. \end{aligned}\right\} \tag{4. 7}$$

5. The general expression for the drag on the elliptic cylinder

Next we shall proceed to the discussion on the drag experienced by the elliptic cylinder under consideration. As is well known, two different methods are commonly used in calculating the drag on a solid body immersed in a stream of viscous fluid. Thus, in one method the drag is calculated by summing up the viscous stresses exerted

* Here we make use of the fact that when s is any positive integer, the modified Bessel function $I_s(x)$ can be expressed as:

$$I_s(x) = \frac{1}{2\pi}\int_{-\pi}^{\pi} e^{x\cos\theta}\cos s\theta\, d\theta.$$

(Cf. G. N. Watson, '*Theory of Bessel functions*,' (Cambridge Univ. Press), 2nd ed. (1948), p. 181.)

by the fluid upon the surface of the obstacle, while in the other, it is calculated by applying the theorem of momentum to an infinite mass of fluid surrounding the body.

As shown in a paper (6) by Aoi and one of the present writers (S. T.), when the analysis is based upon Oseen's equations, the former direct method gives the general formula for the drag D per unit span of a cylindrical obstacle in the form:

$$D = -\rho U \int \frac{\partial \phi}{\partial n} ds , \tag{5.1}$$

where integration is taken round the circumferential curve s of the cylinder and $\partial/\partial n$ means differentiation along the outward normal n to s.

On the other hand, the latter indirect method gives

$$D = -\rho U \int \frac{\partial \phi}{\partial n'} ds' , \tag{5.2}$$

where integration is taken round a large closed contour s' everywhere at a great distance from the cylinder and $\partial/\partial n'$ means differentiation along the outward normal n' to s'.

In the case of the elliptic cylinder $\xi=\xi_0$ under consideration, the formula (5.1) becomes

$$D = -\rho U \int_0^{2\pi} \left(\frac{\partial \phi}{\partial \xi}\right)_{\xi=\xi_0} d\eta , \tag{5.3}$$

while the formula (5.2) takes the form:

$$D = -\rho U \int_0^{2\pi} \left(\frac{\partial \phi}{\partial \xi}\right)_{\xi\to\infty} d\eta , \tag{5.4}$$

provided that a large ellipse confocal with the circumferential curve of the cylinder is taken as the closed contour s'.

Thus it is easily found that if use is made of the expression (2.9) for ϕ, the above two formulae (5.3) and (5.4) lead to one and the same result for the drag on the cylinder, namely:

$$D = -2\pi\rho c U^2 b_0 , \tag{5.5}$$

which, by the aid of equation (3.13), can also be written in the form:

$$D = \frac{\pi\rho U^2}{k} \sigma \sum_{m=0}^{\infty} \lambda_{m,1} a_m , \tag{5.6}$$

where $R=2aU/\nu=4ka$ is the Reynolds number. This gives the general expression for the drag on the elliptic cylinder placed parallel to the uniform stream.

If we define the drag coefficient C_D as $C_D=D/(\rho U^2 \cdot 2a)$, we have

$$C_D = \frac{2\pi}{R} \sigma \sum_{m=0}^{\infty} \lambda_{m,1} a_m . \tag{5.7}$$

6. An expansion formula for the drag

Starting from the general expression (5.7) for the drag coefficient of the elliptic cylinder, we shall derive an expansion formula in powers of the Reynolds number which may be conveniently used for numerical computations of the values of the drag coefficient.

To this end, we have first to determine the a_m's by solving the system of simultaneous linear algebraic equations (3.11). Theoretically the solution of this system of equations has to be obtained by means of infinite determinants, but for the purpose of deriving an expansion formula in powers of the Reynolds number R for the drag coefficient it is necessary and sufficient to find the values of the first few of the a_m's. In fact, it is readily justified that if we confine ourselves to the derivation of an expansion formula correct to the order of R^2, it is necessary and sufficient to determine the first two of the a_m's, namely a_0 and a_1, by solving the following system of three linear algebraic equations:

$$\left.\begin{aligned} &\lambda_{0,2}a_0 + \lambda_{1,2}a_1 + \lambda_{2,2}a_2 = 2q\,, \\ &\lambda_{0,3}a_0 + \lambda_{1,3}a_1 + \lambda_{2,3}a_2 = 0\,, \\ &\lambda_{0,4}a_0 + \lambda_{1,4}a_1 + \lambda_{2,4}a_2 = 0\,, \end{aligned}\right\} \tag{6.1}$$

and in this case the drag coefficient C_D is given by

$$C_D = \frac{2\pi}{R}\sigma(\lambda_{0,1}a_0 + \lambda_{1,1}a_1)\,. \tag{6.2}$$

Using the series expansions for the modified Bessel functions I_s and K_s, the expansions in powers of $q\left(=\frac{1}{2}kc\right)$ have been calculated for the nine $\lambda_{m,n}$'s in (6.1). If we denote for brevity

$$S_1 = -\left\{\gamma + \log\left(\frac{1}{2}\sigma q\right)\right\} = -\left\{\gamma + \log\left(\frac{a+b}{a}\frac{R}{16}\right)\right\}, \tag{6.3}$$

where $\gamma = 0.57721\cdots$ is Euler's constant, the results are as follows:

$$\lambda_{0,1} = \tau - \frac{1}{8}\left\{(\sigma^3 + 4\sigma - 3\tau) + 4\sigma^3 S_1\right\}q^2 + \cdots,$$

$$\lambda_{0,2} = \frac{1}{2}\left\{(1+\tau^2) + 2S_1\right\}q - \frac{1}{48}\left\{(\sigma^4 + 4\tau^2 + 3\tau^4) + 6(\sigma^4 - \tau^4)S_1\right\}q^3 + \cdots,$$

$$\lambda_{0,3} = \frac{1}{8}\left\{(\sigma + 4\tau + \tau^3) + 4\sigma S_1\right\}q^2 + \cdots,$$

$$\lambda_{0,4} = \frac{1}{48}\left\{(\sigma^2 + 9 + 9\tau^2 + \tau^4) + 6(\sigma^2 + 2 - \tau^2)S_1\right\}q^3 + \cdots;$$

$$\lambda_{1,1} = -\frac{1}{2}(\sigma - 2\tau) + \cdots,$$

$$\lambda_{1,2} = \frac{1}{4}\left\{-(\sigma^2 - 2 - \tau^2) + 2S_1\right\}q + \cdots,$$

$$\lambda_{1,3} = \frac{1}{2}\tau + \cdots,$$

$$\lambda_{1,4} = \frac{1}{8}(2 + \tau^2)q + \cdots;$$

$$\lambda_{2,2} = -(1 + \tau^4)\frac{1}{q} + \cdots,$$

$$\lambda_{2,3} = -\frac{1}{6}(3\sigma - 4\tau + 2\tau^5) + \cdots,$$

$$\lambda_{2,4} = \tau^2\frac{1}{q} + \cdots.$$

Making use of these expansions, the system of simultaneous linear algebraic equations (6. 1) has been solved for a_0 and a_1, and substituting the values of a_0 and a_1 thus obtained into the right-hand side of (6. 2) and bearing in mind that

$$q^2 = \frac{k^2c^2}{4} = \frac{R^2}{64}\frac{c^2}{a^2}, \quad R = 4ka,$$

and

$$c\sigma = ce^{\xi_0} = a + b, \quad c\tau = ce^{-\xi_0} = a - b, \quad c^2 = a^2 - b^2,$$

we have calculated an expansion formula for the drag coefficient C_D correct to the order of R^2. The result is given by

$$C_D = \frac{4\pi}{R[S_1 + a/(a+b)]}\left[1 - \frac{1}{S_1 + a/(a+b)}\left\{\left(\frac{a+b}{a}\right)^2 S_1^2 + \frac{a^2+b^2}{a^2}S_1 - \frac{5a^4 - 8a^3b - 30a^2b^2 - 24ab^3 - 3b^4}{12a^2(a+b)^2}\right\}\frac{R^2}{128}\right]. \tag{6.4}$$

This formula differs from the corresponding Sidrak's formula in the coefficient of R^2, but is in complete agreement with the second approximation of Tomotika and Aoi's expansion formula (5).

The above expansion formula may be put in a somewhat simpler form. Thus, denoting

$$\varepsilon = \frac{a-b}{a+b}, \tag{6.5}$$

and

$$S = S_1 + \frac{a}{a+b} = S_1 + \frac{1}{2}(1 + \varepsilon), \tag{6.6}$$

we have

$$C_D = \frac{4\pi}{RS}\left[1 - \frac{1}{(1+\varepsilon)^2 S}\left\{S^2 + \frac{1}{2}(\varepsilon^2 - 2\varepsilon - 1)S - \frac{1}{48}(\varepsilon^4 + 12\varepsilon^3 + 18\varepsilon^2 + 4\varepsilon - 15)\right\}\frac{R^2}{32}\right], \quad (6.7)$$

where

$$S = \frac{1}{2}(1+\varepsilon) - \left\{\gamma + \log\frac{R}{8(1+\varepsilon)}\right\}, \quad \varepsilon = \frac{a-b}{a+b}. \quad (6.8)$$

As the limiting cases of the above formula, we can immediately obtain the expansion formulae correct to the order of R^2 for the drag coefficient of a circular cylinder and of a flat plate placed edgeways along the uniform stream.

(*a*) *The case of a circular cylinder*

Putting $a=b$ in (6.4) or $\varepsilon=0$ in (6.7), we have

$$C_D = \frac{4\pi}{RS}\left[1 - \frac{1}{S}\left(S^2 - \frac{1}{2}S + \frac{5}{16}\right)\frac{R^2}{32}\right], \quad (6.9)$$

where

$$S = \frac{1}{2} - \gamma - \log\frac{1}{8}R. \quad (6.10)$$

This is in accord with the second approximation of Tomotika and Aoi's expansion formula (**7**, **8**) for the drag coefficient of the circular cylinder.

(*b*) *The case of a flat plate*

Putting $b=0$ in (6.4) or $\varepsilon=1$ in (6.7), we obtain the result that

$$C_D = \frac{4\pi}{RS}\left[1 - \frac{1}{S}\left(S^2 - S - \frac{5}{12}\right)\frac{R^2}{32}\right], \quad (6.11)$$

where

$$S = 1 - \gamma - \log\frac{1}{16}R. \quad (6.12)$$

This coincides exactly with what has been given by Piercy and Winny (**9**, **10**).

REFERENCES

1. W. J. Harrison, 'On the motion of spheres, circular and elliptic cylinders through viscous liquid', *Trans. Cambridge Phil. Soc.*, **23** (1924), 71.
2. D. Meksyn, 'Solution of Oseen's equations for an inclined elliptic cylinder in a viscous fluid', *Proc. Roy. Soc.* A, **162** (1937), 232.
3. T. Lewis, 'Solutions of Oseen's extended equations for circular and elliptic cylinders and a flat plate', *Quart. Journ. Math.*, Oxford Series, **9** (1938), 21.
4. S. Sidrak, 'The flow of a viscous liquid past an elliptic cylinder', *Proc. Roy. Irish Acad.*, **53** (1950), 65.
5. S. Tomotika and T. Aoi, 'The steady flow of a viscous fluid past an elliptic cylinder and a flat plate at small Reynolds numbers', To appear soon in *Quart. Journ. Mech. and Applied Math.*

6. S. Tomotika and T. Aoi, 'The steady flow of a viscous fluid past a sphere and circular cylinder at small Reynolds numbers', *Quart. Journ. Mech. and Applied Math.*, **2** (1950), 140.
7. S. Tomotika and T. Aoi, 'An expansion formula for the drag on a circular cylinder moving through a viscous fluid at small Reynolds numbers', *Quart. Journ. Mech. and Applied Math.*, **4** (1951), 401.
8. S. Tomotika and T. Aoi, 'Note on the drag experienced by a circular cylinder moving in a viscous fluid at small Reynolds numbers', *Memoirs Coll. Sci. Univ. of Kyoto*, **26** (1950), 183.
9. N. A. V. Piercy and H. F. Winny, 'The skin friction of flat plates to Oseen's approximation', *Proc. Roy. Soc.* A, **140** (1933), 543.
10. S. Tomotika, 'A note on the skin friction of a flat plate to Oseen's approximation', *Memoirs Coll. Sci., Univ. of Kyoto*, **27** (1953), 1.

Memoirs of the College of Science, University of Kyoto, Series A,
Vol. XXVII, No. 1, Article 3, 1953

ON THE GLIDE TWINNING IN SINGLE CRYSTALS OF TIN

BY

Hiroshi KIHÔ and Ken-ichiro ISHII

(*Received January 29, 1951*)

ABSTRACT

By measuring the energy and the critical shearing stress simultaneously, the mechanism of glide twinning in single crystals of tin has been investigated experimentally by the use of a method first devised by B.Chalmers and somewhat improved by the present writers.

The results obtained varied from specimen to specimen, ranging from 0.9×10^6 to 4.4×10^6 ergs/cc for the energy and from 23 to 61 kg/cm^2 for the critical shearing stress. Plotting the energy against the critical shearing stress, it has been found that there holds a relation $E = \frac{1}{2}eS$, where E is the energy for twinning per unit volume, e the magnitude of shear (being 0.12 in our experiment), and S the critical shearing stress for twinning.

1. Introduction

In 1935, Chalmers (1) made some researches on the mechanical twinning of single crystals of white tin, and estimated the energy necessary for twinning by a method which consisted in comparison of the amplitude of a pendulum of the specimen when it twinned on impact with that when it did not twin.

The present writers have made some improvements upon his method, and a simple relationship between the energy necessary for twinning and the critical shearing stress for twinning by impact has been obtained.

2. Description of the experiments

i) *Experimental procedure*

A number of single crystals of white tin, cylindrical in form, 6mm in diameter and about 3cm in length, were prepared by the method of drawing up a seed crystal from the melt. The orientation of the seed crystal was so arranged that there was only one kind of twinning plane in the specimen. The purity of the specimen was only of commercial, although pure enough to make single crystals of it. After the orientation of the crystal was checked by the optical method, the specimen was set in the pendulum of specimen-holder and struck on one end by a striking pendulum of the same weight, as was done in Chalmer's experiment (Fig. 1).

From the amplitude measured on a scale set closely to the both pendulums the velocities just before and after the collision were estimated. An example of the results is shown in Fig. 2, where the abscissa represents the velocity of the striker, while the ordinate denotes the velocity of the specimen.

As the velocity of the striker is increased, the velocity of the specimen increases linearly, and when the velocity of the striker reaches a certain definite value, say V_0,

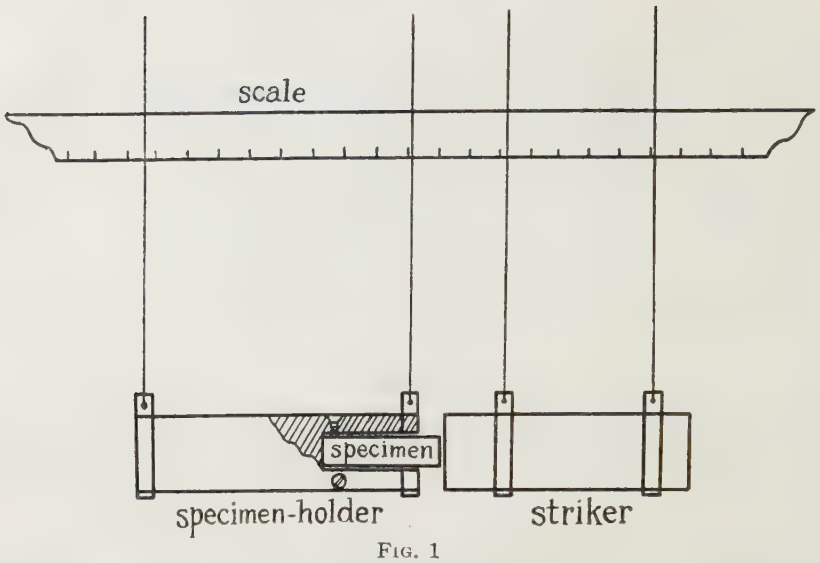

FIG. 1

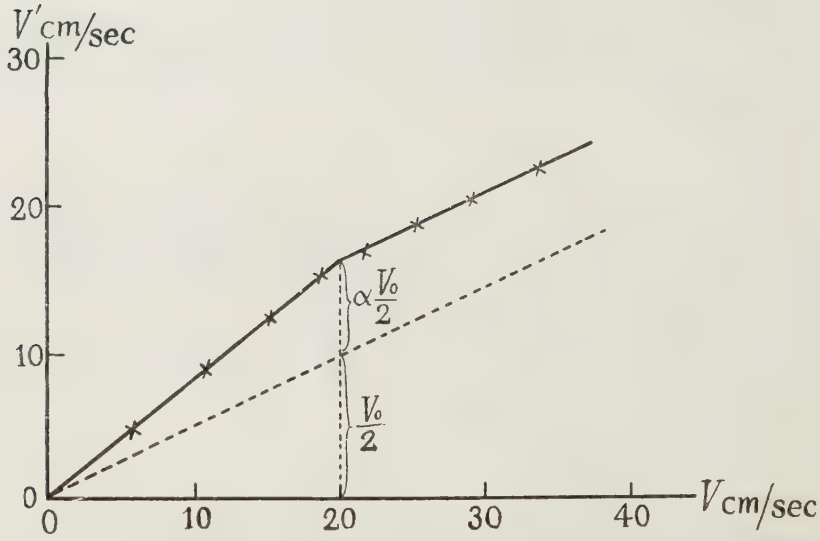

FIG. 2 The relation between the velocities of the striker and the specimen-holder

twinning begins to take place, after which the velocity of the specimen is seen to increase at the gradient of ½ to the velocity V of the striker, as will be seen from the figure.

ii) *Velocity changes by collision*

In order to explain such a relation, we shall for the time being consider a case in which both the pendulums collide on one another with equal speed of $V/2$, which is half the velocity of the striker in our experiment. This is equivalent to a case in which we are observing the collision in our experiment from a coordinate-system moving with the velocity $V/2$ parallel to the velocity of the striker.

In such a case, the two pendulums will repulse one another at the speed $\alpha V/2$, where α is the coefficient of repulsion in the elastic range. As the speed of the two

pendulums, approaching one another, is increased, the collision will become stronger, and at a certain definite velocity, say V_0 2, the collision will become inelastic, and twinning will begin to take place. While the twinning is proceeding, the residual kinetic energy, which will exist if the velocity $V/2$ is larger than $V_0/2$, will be consumed in the work of twinning, and when all of the kinetic energy have been consumed, twinning will stop, and the elastic energy stored in the pendulums will be turned into the kinetic energy of repulsion: the velocity of repulsion after twinning will correspond to the elastic energy at its elastic limit.

Turning now to our case in which the velocity of the striker is V and the specimen-holder is situated at its lowest position, the velocity of the specimen V' after collision will be represented by adding $V/2$ to the velocity of the specimen in the case considered above. Thus,

$$V' = \frac{1}{2}V + \alpha\frac{1}{2}V = \frac{1}{2}(1 + \alpha)V \qquad (1)$$

in the elastic range,

$$V' = \frac{1}{2}V_0 + \alpha\frac{1}{2}V_0 = \frac{1}{2}(1 + \alpha)V_0 \qquad (2)$$

at the elastic limit, and

$$V' = \frac{1}{2}V + \alpha\frac{1}{2}V_0\,, \qquad (3)$$

when twinning occurs.

On the other hand, the velocity of the striker will be equal to the difference of the initial velocity and the velocity of the specimen after collision, preserving the law of conservation of momentum.

iii) *The energy loss by twinning*

From the relations thus obtained, the energy necessary for twinning may be estimated as follows:

The energy-loss by collision will be equal to the difference of the kinetic energies of the system before and after collision, but the energy-loss which exists in the course of the elastic process, i. e., in the elastic compression before twinning and elastic expansion after twinning, should be subtracted from the total energy-loss, in order to estimate the energy-loss by twinning.

If we assume that the energy-loss in the elastic process is equal to that by the collision at V_0, i. e., at the elastic limit, this will be expressed as

$$\frac{1}{2}MV_0^2 - \frac{1}{2}M\left\{(1 + \alpha)\frac{V_0}{2}\right\}^2 - \frac{1}{2}M\left\{(1 - \alpha)\frac{V_0}{2}\right\}^2,$$

in which the first term is the energy of the striker before collision, while the second and third terms are those of the specimen and the striker after collision respectively.

Then the energy-loss E by twinning is given by

$$E = \frac{1}{2}MV^2 - \frac{1}{2}M\left\{\left(\frac{V}{2} + \alpha\frac{V_0}{2}\right)^2 + \left(\frac{V}{2} - \alpha\frac{V_0}{2}\right)^2\right\}$$

$$- \frac{1}{2}MV_0^2 + \frac{1}{2}M\left\{(1 + \alpha)\frac{V_0}{2}\right\}^2 + \frac{1}{2}M\left\{(1 - \alpha)\frac{V_0}{2}\right\}^2$$

$$= \frac{1}{4}M(V^2 - V_0^2)\,. \tag{4}$$

In the earlier experiment by Chalmers, the energy-loss was estimated to be the difference between the amplitude of the specimen when it twinned and that when it did not twin, the initial amplitude having been the same in both cases.

Since, however, the cofficient of repulsion is nearly constant, the energy-loss by the elastic repulsion will increase rapidly with the incident velocity of the striker, so that the result will become less than our result which is obtained under the assumption that the energy-loss is estimated to be the difference of the initial energy of the striker and the energy of the specimen after twinned.

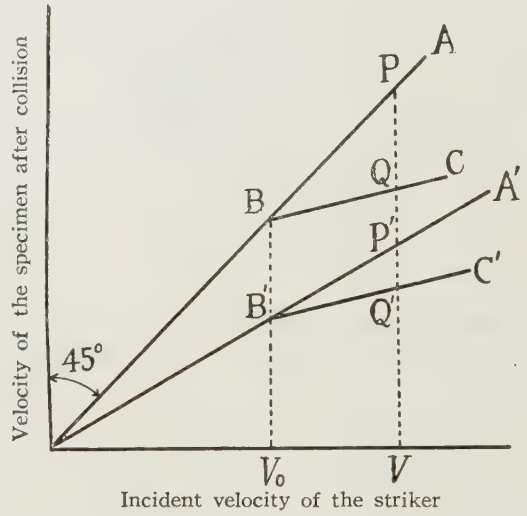

Fig. 3

Fig. 3 explains such circumstances, where the abscissa represents the incident velocity of the striker, while the ordinate is the velocity of the specimen after repulsion. The velocity of the specimen after a perfectly elastic repulsion will be represented by the straight line OA, while the velocity after the actual repulsion by OA′. The velocity after twinning is represented by BC in the perfect case, and by B′C′ in the actual case, and when twinning have occurred at the incident velocity V, the total energy-loss by collision will correspond to the velocity difference PQ′ in the figure, and since we have assumed in the above that the energy-loss in the elastic process by twinning is equal to that at the critical point V_0, this will correspond to QQ′ (= BB′), and thus the energy-loss by twinning will correspond to PQ (= PQ′ − QQ′) in our method.

On the other hand, according to the earlier method the energy-loss by twinning will correspond to P′Q′.

Quantitatively, according to the earlier method the energy-loss will become

$$E = \frac{1}{2}M\left[\left\{(1+\alpha)\frac{V}{2}\right\}^2 + \left\{(1-\alpha)\frac{V}{2}\right\}^2\right]$$

$$- \frac{1}{2}M\left[\left\{\frac{V}{2} + \alpha\frac{V_0}{2}\right\}^2 + \left\{\frac{V}{2} - \alpha\frac{V_0}{2}\right\}^2\right]$$

$$= \frac{1}{4} M\alpha^2(V^2 - V_0^2)\,, \qquad (5)$$

since the velocity of the specimen will be $(V + V_0/2)$ when the specimen twinned and $(1 + \alpha)V/2$ when it did not twin.

The value of α observed in the experiment is approximately 0.6, so that the result obtained from (5) will become about one-third of that obtained from (4). As will be seen in Table I, this is in fact the case, since the mean value of the energy-loss obtained by Chalmers was 8×10^5 ergs/cc, while it ranges from 0.9×10^6 to 4.4×10^6 ergs/cc in our experiment.

iv) *The critical shearing stress*

The critical shearing stress for twinning will be estimated on the ground that the elastic energy stored in the pendulum is changed into the kinetic energy of repulsion.

We may assume that most of the elastic energy is stored in the tiny specimen of single crystal of tin attached to the front of the specimen-holder, because the cross-section of the specimen is about one-tenth of the cross-section of both the specimen-holder and the striker, and the elastic constants are smaller than that for iron, so that the compression will take place mainly in the specimen.

If we denote the volume of the specimen by V_s, the normal pressure at the elastic limit by P and the compressibility of the specimen along the direction of the specimen axis by k, the energy stored in the specimen at the elastic limit will be equal to $V_s P^2 (2k)$, and since this should be equal to the kinetic energy of the two pendulums, as is considered in ii), we obtain the relation:

$$\frac{V_s P^2}{2k} = 2 \times \frac{1}{2} M\left(\frac{\alpha}{\alpha'} V_0\right)^2,$$

or

$$P = \sqrt{\frac{2M}{kV_s}} \frac{\alpha}{\alpha'} V_0\,, \qquad (6)$$

where M is the mass of each pendulum and α' is a correction factor due to the fact that a part of the elastic energy must have been dissipated during the elastic expansion and that some of the elastic energy stored both in the specimen-holder and the striker must contribute to the velocity after collision.

The critical shearing stress which is denoted by S_c will be obtained from P by the relation:

$$S_c = P \cos\theta \cos\psi\,, \qquad (7)$$

where θ is the angle between the axis of the specimen and the normal to the twinning plane and ψ the angle between the specimen-axis and the direction of twinning.

The compressibility k will be obtained from the elastic parameters for white tin as

$$k = (l^4 + m^4)c_{11} + n^4 c_{33} + l^2 m^2(2c_{12} + c_{66}) + n^2(l^2 + m^2)(2c_{13} + c_{44})\,, \qquad (8)$$

where l, m and n are the direction-cosines of the specimen-axis referred to the a, b and c axes of the crystal.

As to the correction factor α', it will be adequate to estimate it to be nearly 0.8, if we neglect the effect of the striker and the holder, because the value of α', being a part of the coefficient of repulsion concerning only the elastic expansion, will not be far from $\sqrt{\alpha}$, where α is 0.6 or 0.65 in our experiment. Taking account of the

effect of the striker and the holder, the value of α' would be a little larger than 0.8.

The critical shearing stress by static compression may not be utilized, since it might depend upon the speed of compression, at any rate.

3. Results of experiments

i) *The energy-loss and the critical shearing stress*

As already mentioned, the mean value obtained for the energy was approximately 3×10^6 ergs/cc and varied from 0.9×10^6 to 4.4×10^6 ergs/cc. On the other hand, the critical shearing stress for twinning also varied from specimen to specimen, ranging from 23 to 61 kg/cm^2. The details are shown in Table I below.

TABLE I

No.	$E \times 10^5$ ergs	V_t cc	$E/V_t \times 10^6$ ergs/cc	$\alpha' P$ kg/cm^2	$\alpha' S_c$ kg/cm^2	orientation θ	orientation ϕ
1	10.9	0.4	2.5	102	39	57	47
2	4.7	0.3	1.6	60	23	〃	〃
3	2.6	0.17	0.9	61	28	48	47
4	9.4	0.26	3.6	114	52	〃	〃
5	3.6	0.12	2.9	93	42	〃	〃
6	6.7	0.24	2.8	94	42	〃	〃
7	5.1	0.12	4.2	135	61	〃	〃
8	7.8	0.23	3.6	105	47	〃	〃
9	7.8	0.18	4.2	108	49	〃	〃
10	6.3	0.15	4.2	130	59	〃	〃
11	7.0	0.37	1.9	110	51	〃	〃
12	16.6	0.38	4.4	108	49	〃	〃

E is the total energy-loss by twinning and V_t is the volume twinned for each specimen. In the fifth and sixth columns, α' is not removed, because it is not yet determined exactly.

ii) *A relation between the energy-loss and the critical searing stress*

As is shown in Fig. 4, a linear relation is obtained by plotting the energy-loss against

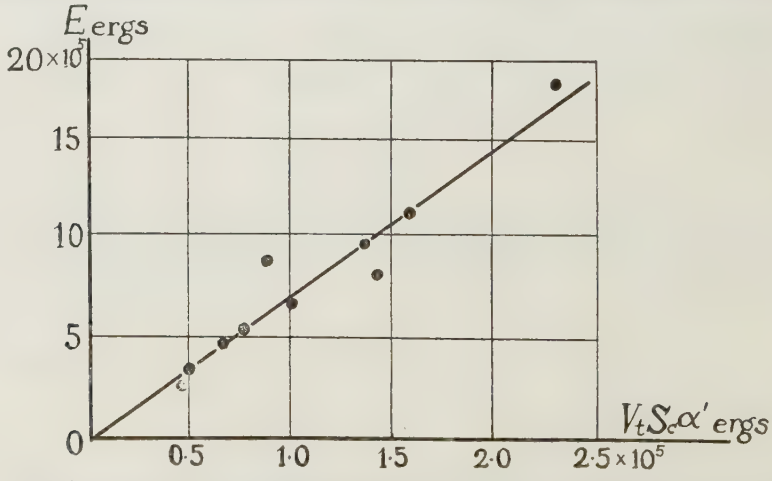

FIG. 4 Experimental results representing the linear relation between the energy-loss by twinning and the product of the volume twinned V_t, the critical shearing stress S_c.

the product of V_t and $\alpha' S_c$. This will be expressed as:

$$E = 0.07 V_t a' S_c ,$$

and, since the magnitude of shear e is 0.12 for the twinning of white tin, this becomes

$$E = \frac{1}{2} e V_t \left(\frac{a'}{0.9}\right) S_c ,$$

or approximately

$$E = \frac{1}{2} V_t S_c , \tag{9}$$

for, as was already mentioned in iv), α' is equal to, or a little larger than, 0.8.

If, on the other hand, we consider that the energy is consumed against the friction between the gliding plane and the underlying plane, the energy-loss will be expressed as:

$$E = e V_t S , \tag{10}$$

where S represents the friction per unit area, since the product eV_t is equal to the product of total area of twinning lattice planes and its displacement.

From (9) and (10) we obtain a relation that

$$S = \frac{1}{2} S_c . \tag{11}$$

Returning to (9), if ε is the energy-loss, f the critical shearing stress each for one atom twinned, and d the distance between the original and its twinned lattice point, it is easily found that the relation (9) is translated into

$$\varepsilon = \frac{1}{2} f d , \tag{12}$$

which shows that the friction during the process of twinning is one-half of the critical shearing stress.

If the above relation (12), which is directly translated into microscopic terms, is to be correct, this may be interpreted schematically in such a way that there is a potential barrier of height ε between the original and the twinned sites and a straight potential gradient f from the original site to the top of the potential barrier. But this should not be accepted directly, since ε is much less than the energy of thermal vibration kT, which is about 4×10^{-14} ergs at room temperatures, while ε is nearly equal to 8×10^{-17} ergs.

An alternative description may be made by assuming that ε is again equal to the energy of activation: the rate of twinning will be roughly proportional to

$$\left[\exp\left\{-\left(\varepsilon - \frac{1}{2} df\right)\Big/ kT\right\}\right]^n ,$$

or

$$= \exp\left\{-n\left(\varepsilon - \frac{1}{2} df\right)\Big/ kT\right\} ,$$

if we assume that n atoms will twin simultaneously. Since n will be a large number,

the exponential will be infinitesimal when $df/2 < \varepsilon$, but will become enormously large as soon as $df/2$ exceeds ε. This seems to explain the step-wise characteristics of mechanical twinning as well as the above relation (12).

The examinations on the temperature dependency of the results and on the variation of the critical shearing stress for twinning are now being continued, of which we may report shortly.

In conclusion, the writers express their sincere thanks to Professor K. Tanaka for his kind guidance throughout the present experiments. The present study is supported by a grant-in-aid of the Ministry of Education.

REFERENCE

1. B. Chalmers, *Proc. Phys. Soc.* **47** (1935), 733.

Memoirs of the College of Science. University of Kyoto, Series A,
Vol. XXVII, No. 1, Article 4, 1953

ON A NEW METHOD OF MEASURING SPECIFIC HEAT OF METALS*

BY

Shigeka NISHIOKA

(*Received March 15, 1951*)

ABSTRACT

The direct heating method of measuring the true specific heat of metals has been improved. The details of apparatus and experimental procedure are given. The accuracy of the present method is shown in detail with the experimental data for copper. The advantages of the present method lie in the considerable precision and speediness.

1. Introduction

For the determination of specific heat of metals, a method has been adopted by Jaeger and Diesselhorst (1) and others (2–5) in which specimens in the form of a rod or a wire are heated directly by an electric current. In this method the temperature is measured usually by thermo-couples or resistance thermometers. The writer has tried to develop a new method in which the temperature is determined by measuring the linear expansion of the specimen. The advantages of the present method lie in its precision and speediness.

2. Theory of the method

Now consider the ideal case of a uniform wire of metal exposed to the air held at constant temperature θ_0. Let ρ and r be the mass and the resistance of the wire per unit length respectively, and also let p, c and h be the perimeter, the specific heat and the surface emissivity of the wire respectively. Further, let an electric current of intensity I flow through the wire. Then the temperature θ of the wire at any time t will be given by the equation:

$$\rho c d\theta = \frac{I^2 r}{J} dt - ph(\theta - \theta_0)\, dt\,, \tag{1}$$

where J is the mechanical equivalent of heat. In the following lines, the dimensions, temperatures, times and heat quantities are expressed in centimeters, degrees, Centigrade, seconds and calories respectively.

On integration the solution of equation (1) may be written as:

$$\theta - \theta_0 = \frac{I^2 rt}{J\rho c}\left\{1 - \frac{1}{2}\frac{pht}{\rho c} + \frac{1}{6}\left(\frac{pht}{\rho c}\right)^2 - \cdots\right\}. \tag{2}$$

If the time t is small and the surface of the wire is polished sufficiently in order to diminish the emissivity, the term $\frac{1}{6}(pht/\rho c)^2$ in equation (2) may be neglected in

* Communicated by Professor S. Tomotika.

comparison with the first two terms. For example, if the wire is of copper, and $t = 8$, $h = 0.0003$ and $p = 0.9$, the value of $\frac{1}{6}(pht/\rho c)^2$ becomes 0.0001. Thus, equation (2) may now be written as:

$$\theta - \theta_0 = \frac{I^2 rt}{J\rho c}\left(1 - \frac{pht}{2\rho c}\right). \tag{3}$$

Therefore it is seen that the temperature-excess $(\theta - \theta_0)$ is represented by a quadratic function of the time t. Since, over a short range of temperature, the magnitude of thermal expansion is proportional to the increase of temperature, the linear expansion l of the wire per unit length at the time t may be expressed as follows:

$$l = At + Bt^2 ,$$

where A and B are constants. If the thermal expansions at t_1 and t_2 are denoted by l_1 and l_2 respectively, we have

$$\left|\frac{dl}{dt}\right|_0 = A = \frac{l_1 t_2^2 - l_2 t_1^2}{t_1 t_2 (t_2 - t_1)}, \tag{4}$$

where $|dl/dt|_0$ is the ratio at $t = 0$ of the linear expansion per unit length to the time, at which the heat-loss from the surface of the wire is nil. The temperature-rise $\Delta\theta$ per unit time is equal to A/α, where α is the coefficient of linear expansion, provided that the heat-loss is nil. Therefore the specific heat c is calculated from the formula:

$$c = \frac{I^2 r}{J\rho\Delta\theta} = \frac{I^2 r\alpha}{J\rho A}. \tag{5}$$

3. Apparatus and experimental procedure

The arrangement of the apparatus is shown in Fig. 1. S is the specimen in the form of a uniform wire, the both ends of which being bent rectangularly and immersed in mercury cups. The specimen rests upon a knife edge K and upon a roller with a mirror, the roller resting upon a horizontal flat plate too. S′ is a wire of the same

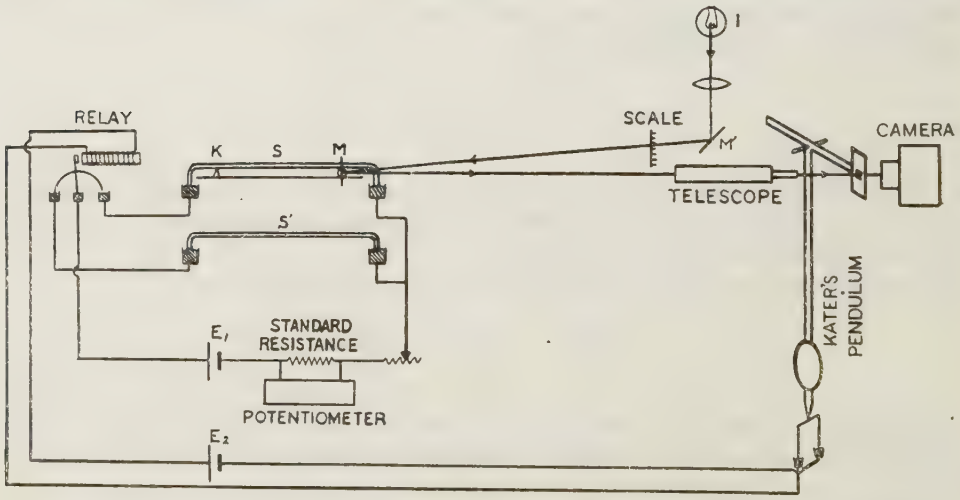

Fig. 1

material and shape as S.

The electric circuits connecting the battery E_1, the standard resistance, the potentiometer, S and S′ are shown in Fig. 1. The electric current flowing through S′ is capable of being exchanged to S by means of a relay which works at an instant at which Kater's pendulum comes to the vertical position and passes through the mercury contact. The intensity of electric current can be determined by means of the standard resistance and the potentiometer. The light started from the lamp I passes through the scale and then is reflected at the mirror M and again passes through the telescope with a cross-wire and through a hole in a plate which is attached to Kater's pendulum, and enters finally into the camera. The light can pass through the hole when and only when the pendulum comes to the vertical position.

At the beginning of the observation, the pendulum is inclined so that the light is obstructed to enter into the camera, and the electric current flows through S′. After a few minutes, when the electric current has become steady, the pendulum is started. When it comes to the vertical position, the light enters into the camera through the hole and the images of the scale and the cross-wire are photographed, and at the same time the electric current is exchanged from S′ to S. After t_1 and t_2 seconds, the light is made to enter into the camera separately, photographing the displacement of the image of the scale at each time, and thus the thermal expansions l_1 and l_2 for the time intervals t_1 and t_2 respectively are calculated. Thus the value of $|dl/dt|_0$ is obtained by equation (4). At the same time the intensity of the electric current is measured, while the resistance and the coefficient of thermal expansion are determined by separate experiments.

4. Sources of error

(1) If the length of the wire of specimen is too short, the temperature-rise at the centre becomes larger than the one at the end, and heat flows along the length of the wire, which gives rise to an error, especially when the specimen is of a good conductor. The appropriate length of the wire is so determined experimentally that the temperature at any point on the specimen may rise equally when it is heated by electric current.

(2) When the temperature-excess is too large and the radius of the wire is too small, Newton's law will not be applicable.

(3) When the time interval of heating is too long and the radius of the wire is too small, the heat-loss from the surface becomes large in comparison with the heat quantity used to raise the temperature of the wire, as is evident from equation (3), and consequently the experimental error may increase.

(4) If the temperature of the surrounding atmosphere is not constant, a correction is needed. For example, when the temperature of the surrounding atmosphere is ascending, the thermal expansion due to its effect for the time t_1 must be subtracted from l_1 in equation (4).

5. Precision of the method

The precision of the present method will be shown, taking, as an example, the measurements for electrolytic copper. The specimens in the form of uniform wire of 2.9 mm in diameter were annealed in vacuum at the temperature 550° for 30 minutes and then cooled down slowly to the room temperature. With three specimens, eighteen measurements were carried out. The detailed experimental data for one typical measurement are shown below. The results of all our measurements are given in Table II.

Typical experimental data

Mean temperature of the specimen during the experiment: 30.5°,
Distance between the mirror and the scale: 78.65 cm,
Length of the specimen between the knife-edge and the axis of the roller: 17.51 cm,
Diameter of the roller: 0.2643 cm,
Period of Kater's pendulum (T): 2.379 sec,
$t_1 = 4T$, $t_2 = 8T$, $l_1 = 0.9448 \times 10^{-5}$ cm, $l_2 = 1.8437 \times 10^{-5}$ cm,
$A = 1.0170 \times 10^{-6}$ cm/sec, $I = 22.57$ ampere, $\alpha = 0.00001651$,
$r = 0.00002733$ ohm/cm, $J = 4.185$, $\rho = 0.5868$ gr/cm, $\Delta\theta = 0.06159°$,
$c = I^2r/(J\rho\Delta\theta) = 0.09205$.

TABLE I

Specimen No. 1		Specimen No. 2		Specimen No. 3	
Temp.	Specific heat	Temp.	Specific heat	Temp.	Specific heat
26.9°	0.09186	26.7°	0.09201	26.1°	0.09206
26.3	9177	26.8	9160	26.7	9191
28.0	9201	27.4	9166	28.2	9172
28.9	9180	28.2	9189	29.0	9183
30.5	9164	31.6	9206	31.1	9233
30.5	9205	31.3	9202	30.2	9171
Mean 28.5	0.09186	28.7	0.09187	28.6	0.09193

The specific heat at 28.6° is 0.09189 ± 0.00004, the experimental error being 0.03%. The true values of specific heat for copper obtained by other authors are summarized in Table II, where the "specific heat at 18°" is the modified value obtained from the observed one by assuming that the temperature coefficient of specific heat is 0.00041 (**6**).

The present writer measured also the specific heats of constantan and brass by making use of the same method. The experimental error of these measurements was about 0.05% which shows better precision of the present method in comparison with those obtainable by the method of mixture or cooling.

TABLE II

Experimenter	Specific heat observed	Specific heat at 18°	
Gaede (**7**)	0.09108 at 16.7°	0.09113	0.09143
Griffith (**8**)	0.09159 at 14.21°	0.09174	
Harper (**2**)	0.0915 at 20°	0.09142	
Present writer	0.09189 at 28.6°	0.09145	

REFERENCES

1. JAEGER und DIESSELHORST, *Wiss. Abh. d. Phys. Tech. Reich.*, **3** (1900), 269.
2. HARPER, *Bull. Bureau of Standards*, **11** (1915), 259.
3. PIRANI, *Verh. d. Phys. Gesells.*, **14** (1912), 1037.
4. WORSHING, *Phys. Rev.*, **12** (1918), 199.
5. CORBINO, *Phys. ZS.*, **14** (1913). 915.
6. International Critical Tables, Vol. V, p. 88.
7. GAEDE, *Phys. ZS.*, **4** (1902), 105.
8. GRIFFITH, *Proc. Roy. Soc.* A, **88** (1913), 549.

Memoirs of the College of Science, University of Kyoto, Series A,
Vol. XXVII, No. 1, Article 5, 1953

EFFECTS OF COLD WORKING ON SPECIFIC HEAT OF METALS*

BY

Shigeka NISHIOKA

(*Received March 15, 1951*)

ABSTRACT

Effects of cold working on the specific heats of constantan, brass and copper have been studied experimentally. It has thus been shown that the effect could not be recognized for the above metals. The effects of cold working on specific resistance, density and thermal expansion have also been investigated for the same metals. Richarz's law as well as Geiss and Liempt's relation have been studied.

1. Introduction

A number of workers have investigated the effects of cold working on the specific heats of copper, nickel, lead, platinum, silver, iron and bronze. The results of these investigations may be summarized as follows:

(1) In many investigations (**1**, **2**, **3**) it was found that the specific heat was increased by nearly 1%. But in some investigations (**4**, **5**) the effect was found to be very small.

(2) The experimental error of these measurements was about 0.5% which is of nearly equal order to the effect of cold working. Therefore, in order to decide the matter, a more precise method must be used.

The object of the present investigation is to study the problem for the case of copper, constantan and brass by using a precise method which is reported in the writer's preceding paper. The principle of the method is that, if an electric current of intensity I flows through a wire, the change occurs in length of the wire by Joule's heat, which determines the ratio A of the linear expansion to the time, and the specific heat c can be calculated by the formula:

$$c = \frac{I^2 r \alpha}{J \rho A}, \qquad (1)$$

where r and ρ are the resistance and the mass per unit length of the wire respectively, J the mechanical equivalent of heat and α the coefficient of linear expansion which is determined by another separate experiment.

2. Case of constantan

The specimen under test is of commercial constantan wire of about 2.64mm in diameter, the constitution of which is Cu 57.5% and Ni 42.5%. Two kinds of specimen were prepared, namely, (1) three specimens of hard constantan, (2) three specimens of soft constantan which were annealed in vacuum for two hours at 1000° and then cooled

* Communicated by Professor S. Tomotika.

down slowly to the room temperature. The measured values of density and specific resistance are given in Table I. The lengths, temperatures, heat quantities and electric resistance are expressed in centimeters, degrees, Centigrade, calories and ohm respectively.

TABLE I

Specimen		Density at 10°		Specific resistance at 14.6°	
Hard	No. 1	8.884	8.878	5.052×10^{-5}	5.059×10^{-5}
	No. 2	8.888		5.058	
	No. 3	8.861		5.068	
Soft	No. 4	8.901	8.899	4.903×10^{-5}	4.902×10^{-5}
	No. 5	8.902		4.900	
	No. 6	8.894		4.904	

As will readily be seen from the above table, the hard constantan is by 0.24% less than the soft one in density and by 3.2% larger in specific resistance.

The linear expansion of the specimen relative to that of fused silica, was determined by using a circular roller with a mirror over the range of temperature from 10° to 100°. The results are expressed by an equation:

$$l_\theta = l_0(1 + 13.94 \times 10^{-6}\theta + 5.2 \times 10^{-9}\theta^2), \qquad (2)$$

where l_θ and l_0 are the length of the wire at θ° and 0° respectively, while the linear expansion of fused silica itself is expressed by the following equation*:

$$l_\theta = l_0(1 + 0.38 \times 10^{-6}\theta + 1.4 \times 10^{-9}\theta^2). \qquad (3)$$

Thus, the linear expansion of hard constantan may be expressed as:

$$l_\theta = l_0(1 + 14.32 \times 10^{-6}\theta + 6.6 \times 10^{-9}\theta^2). \qquad (4)$$

The difference between the linear expansion of the hard constantan and that of soft one was determined directly by using a circular roller with a mirror. The results show that the expansion of the hard constantan is by 0.02% larger than that of the soft one, the error of this measurement being 0.04%.

The specific heat was determined with the formula (1). The results are given in Table II and summarized as follows:

Specific heat of hard constantan at 15°: 0.09768 ± 0.00005.
Specific heat of soft constantan at 15°: 0.09769 ± 0.00005.
Difference: 0.01%.

* The mean value of the results obtained by Chapieus (1903), Scheel (1907), Scheel and Heuse (1914), and Scheel (1921).

TABLE II

Hard constantan			Soft constantan		
Specimen	Temp.	Specific heat	Specimen	Temp.	Specific heat
	15.2	0.09736		13.7	0.09744
	14.2	9755		16.5	9766
No. 1	15.4	9774	No. 4	13.7	9757
	14.6	9789		16.1	9745
				13.8	9732
	15.6	9769		14.7	9736
	14.0	9765		14.2	9772
No. 2	15.1	9766	No. 5	14.6	9743
	16.0	9804		15.8	9773
	9.4	9719		13.9	9795
	18.4	9768		17.0	9812
	16.2	9788		13.9	9760
No. 3	13.6	9739	No. 6	16.1	9819
	11.8	9789		16.5	9805
				9.9	9753
Mean	14.5	0.09766	Mean	14.7	0.09768

3. Case of brass

The specimen of hard brass wire of 5 mm in diameter was prepared by drawing, by which the cross-sectional area was reduced to 50% of its original value. The specimen of soft brass was prepared by annealing in vacuum for 30 minutes at 600°. The constitution was Cu 70% and Zn 30%. The specific resistance and density of the specimens are shown in Table III.

TABLE III

Specimen		Density at 22.5°		Specific resistance at 28°	
Hard	No. 1	8.497	8.489	7.859×10^{-6}	7.853×10^{-6}
	No. 2	8.489		7.823	
	No. 3	8.482		7.876	
Soft	No. 4	8.469	8.469	7.285×10^{-6}	7.302×10^{-6}
	No. 5	8.465		7.325	
	No. 6	8.474		7.296	

The experimental value of the linear expansion for hard brass was found to be expressed as follows:

$$l_\theta = l_0(1 + 17.99 \times 10^{-6}\theta + 7.0 \times 10^{-9}\theta^2).$$

The error of this measurement was 0.04%. The linear expansion of the hard brass was by 0.015% larger than that of the soft one, the error being 0.04%.

The specific heat was determined as in the case of constantan. The results are given in Table IV and summarized as follows:

Specific heat of hard brass at 23°: 0.09073 ± 0.00006.
Specific heat of soft brass at 23° : 0.09072 ± 0.00005.
Difference: 0.01%.

TABLE IV

Hard brass			Soft brass		
Specimen	Temp.	Specific heat	Specimen	Temp.	Specific heat
No. 1	23.3°	0.09072	No. 4	23.5°	0.09030
	24.4	9104		21.9	9088
	22.9	9099		22.9	9052
	22.9	9090		24.9	9028
	23.8	9071		23.4	9073
No. 2	23.1	9056	No. 5	22.6	9126
	21.6	9064		22.6	9086
	22.3	9086		23.6	9091
	24.3	9115		23.1	9090
	24.7	9135		23.5	9110
No. 3	22.7	9065	No. 6	23.7	9067
	23.3	9025		22.3	9032
	23.2	9025		22.7	9086
	22.4	9038		23.0	9081
	23.6	9044		24.5	9036
Mean	23.2	0.09073	Mean	23.2	0.09072

4. Case of copper

The electrolytic copper was used. The specimen of hard copper wire of 2.9 mm in diameter was prepared by drawing, by which the cross-sectional area was reduced to 50% of its original value. The specimen of the soft copper was prepared by annealing in vacuum for 30 minutes at 550°. The experiments were carried out when three months had passed after the preparation of the specimens. The specific resistance and density of the specimens are given in Table V below.

TABLE V

Specimen		Density at 24°		Specific resistance at 26.9°	
Hard	No. 1	8.904	8.907	1.8143×10^{-6}	1.8142×10^{-6}
	No. 2	8.909		1.8144	
	No. 3	8.909		1.8138	
Soft	No. 4	8.903	8.908	1.7814×10^{-6}	1.7803×10^{-6}
	No. 5	8.910		1.7786	
	No. 6	8.910		1.7810	

The experimental value of the linear expansion for the copper was found to be expressed as:

$$l_\theta = l_0(1 + 16.123 \times 10^{-6}\theta + 6.45 \times 10^{-9}\theta^2).$$

The error of this measurement was 0.04%. This linear expansion of the hard copper

was by 0.09% larger than that of the soft one, the error being 0.02%.

The specific heat was determined as in the case of constantan. The results are given in Table VI and summarized as follows:

Specific heat of hard copper at 28.5°: 0.09184 ± 0.00004.

Specific heat of soft copper at 28.5° : 0.09188 ± 0.00004.

Difference: 0.04%.

Table VI

Hard copper			Soft copper		
Specimen	Temp.	Specific heat	Specimen	Temp.	Specific heat
No. 1	26.8°	0.09165	No. 4	26.9°	0.09186
	26.3	9211		26.3	9177
	28.8	9211		28.0	9201
	27.8	9180		28.9	9180
	30.4	9208		30.5	9164
	30.9	9203		30.5	9205
No. 2	25.9	9150	No. 5	26.7	9201
	25.9	9172		26.8	9160
	27.5	9234		27.4	9166
	28.5	9153		28.2	9189
	31.0	9180		31.6	9206
	31.1	9170		31.3	9202
No. 3	26.5	9203	No. 6	26.1	9206
	26.9	9155		26.7	9191
	28.0	9150		28.2	9172
	28.8	9192		29.0	9183
	32.0	9189		31.1	9233
	30.4	9190		30.2	9171
Mean	28.5	0.09184	Mean	28.6	0.09189

5. Summary

(1) The results for constantan, brass and copper are summarized in Table VII.

Table VII

Substance	Δr	Δc	$\Delta \rho$	$\Delta \alpha$
Copper	1.9%	0	− 0.01%	0.09%
Constantan	3.2	0	− 0.24	0
Brass	7.6	0	0.23	0

Δr, Δc, $\Delta \rho$ and $\Delta \alpha$ represent the increase of the specific resistance, the specific heat, the density and the linear expansion due to cold working respectively. The value of increase which is within the experimental error is denoted by zero.

It is well known that the electrical resistance is one of the physical properties which are remarkably affected by cold working and that the change of resistance generally increases as the degree of cold working. Hence the amount of Δr in Table VII indicates the approximate degree of cold working.

TABLE VIII

Experimenter	Kind of working	Increase of specific heat due to cold working
Regnault (6)	Hammering	1.4 %
Kahlbaum, Roth & Siedler (4)	Hammering	very small
Gaudino (2)	Stretching	1.5 %
Jaeger, Rosenbohm & Bottema (3)	Stretching	1 % The effect decreases with the lapse of time and vanishes at last.

(2) As will be seen evidently from Table VII, the changes of the specific heat for copper, constantan and brass are not larger than the experimental error. The results of investigations by other authors for copper are summarized in Table VIII for comparison. There are large discrepancies among the results. Regnault and Gaudino reported considerably large effects in comparison with that of Kahlbaum. It is not considered however that these discrepancies are attributable mainly to the kind and degree of working. The writer could not see the time-effect such as reported by Jaeger. The investigations for constantan and brass have never been published so far.

(3) Geiss and Liempt (7) deduced the following relation and verified its validity for nickel and tungsten:

$$c_k - c_r = \left(\frac{R_k}{R_r} - 1\right)\frac{c_0\beta}{\alpha},$$

where c_k and R_k are the specific heat and specific resistance for metals worked respectively, c_r and R_r are the specific heat and specific resistance of recrystallized metal, c_0 and β the specific heat and temperature coefficient respectively for recrystallized metal at 0°, and α is the temperature coefficient of resistance. It is verified that this relation is not valid for copper, constantan and brass by adopting the values of Δr and Δc in Table VIII and the usual existing data of β and α.

(4) The fact that the specific heat of metals increases with decreasing amount of their density, is known as Richarz's law (9). Schlett (1) verified this relation experimentally using platinum and nickel. As will readily be seen from Table VII, this relation is not applicable to constantan and brass, however.

(5) Jubitz (9) reported that the coefficient of thermal expansion of metals belonging to cubic system is not affected by cold working. The results of the present experiment show that the results for constantan and brass are in good agreement with Jubitz's results, but in the case of copper there occurs an increase of about 0.1%, contrary to Jubitz's results.

REFERENCES

1. SCHLETT, *Ann. d. Phys.*, **26** (1908), 20.
2. GAUDINO, *Rend. di Napoli*, **35** (1924), 204.
3. JAEGER, ROSENBOHM and BOTTEMA, *Proc. Amsterdam.* **35** (1932), 772.
4. KAHLBAUM, ROTH and SIEDLER, *ZS. f. anorg. Chem.*, **29** (1902), 242.
5. CHAPELL and LEWN, *Ferum*, **10** (1912), 271.
6. REGNAULT, *Pogg. Ann.*, **51** (1840), 240.
7. GEISS and LIEMPT, *ZS. f. anorg. Chem.*, **171** (1928), 317.
8. RICHARZ, *Marburger Ber.* (1905), 201.
9. JUBITZ, *ZS. f. tech. Phys.*, **7** (1926), 522.

Memoirs of the College of Science, University of Kyoto, Series A,
Vol. XXVII, No. 1, Article 6, 1953

A NEW METHOD OF MEASURING ULTRASONIC SOUND VELOCITIES IN LIQUIDS

BY

Isao TAKAHASHI, Yoshio ISHIDA and Mitsuo ÔTA

(*Received September 7, 1951*)

1. Introduction

It requires a considerable time to measure ultrasonic sound velocities in liquids either by an interferometer (**1**) or by Debye-Sears's method (**2**). The present authors have devised a new method by which we can finish the measurement in comparatively short time. The principle of our method is explained. When a train of ultrasonic waves traverses a liquid, it forms a kind of grating against the parallel lights. We will call it an ultrasonic grating. We superpose an optical grating on the ultrasonic grating. Then, no changes occur in the diffraction image when the grid constants of the both two are equal, but if the two grid constants are not equal, the image shows some complication. The difference of images can be clearly recognized. We have ascertained experimentally that when we rotate the optical grating around the light path as the axis, its grid constant varies continuously according to the law: $d = d_0 \operatorname{cosec} \theta$. Therefore, by finding the coincidence of the two grid constants we can know from the rotating angle of the optical grating, the grid constant of the ultrasonic grating, i. e. the wavelength of the ultrasonic wave in the liquid. From this value and the frequency, we can determine the ultrasonic sound velocity.

2. Experimental apparatus

The schematic diagram of the experimental apparatus is shown in Fig. 1.

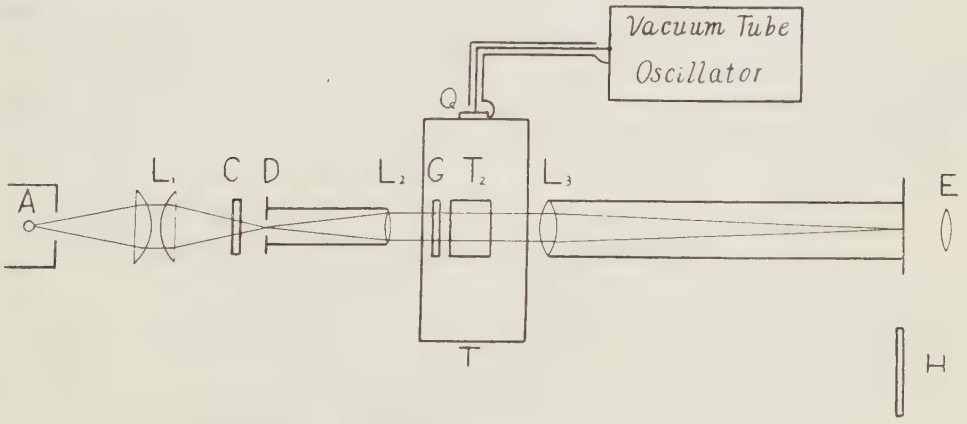

Fig. 1 Experimental apparatus

T_1: Brass trough containing water, whose both sides consist of polished glasses.
T_2: Glass trough, which is used to contain liquid samples.
Glass pieces of the trough are connected by melting glass powder of lower melting temperature inserted at their joints. Therefore, it can hold any organic compounds and strong acids.
A : Light source, mercury arc lamp.
L_1: Condenser lens.
C : Filter which can pass only the green light of mercury spectrum, 5461 Å.
D & L_2, slit and lens respectively, are so adjusted as to make the light rays parallel.
G : Rotatable optical grating, its action being stated later in detail.
Q : Quartz crystal, disk-shaped (diameter 25 mm) cemented over the hole (diameter 12 mm) in one side wall of the brass trough. The resonance frequency 4 Mc/s. It is driven by the vacuum tube oscillator.
L_3: Image forming lens, the focal length being about 1.80 m. The diffraction image can be observed by an eye-piece E or can be photographed by a plate held in H.

3. Rotatable optical grating

The phenomena when an optical grating is rotated, will be considered here. When the grating is set horizontally, i. e. the lines of grating are perpendicular to the slit, the diffraction image does not appear, excepting a central line. If we rotate it by an angle θ from the horizontal position, the image appears as shown in Fig. 2.

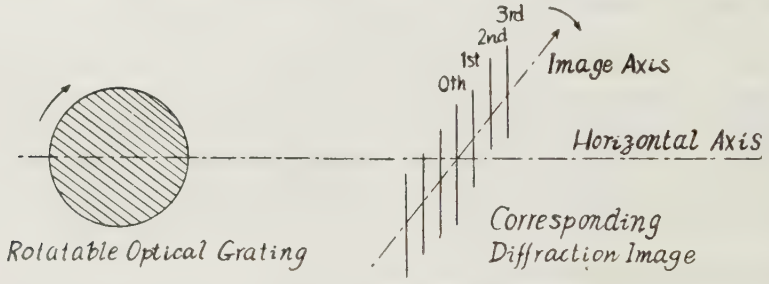

Fig. 2 Effect of rotating the grating

In this case, it is noticeable that the diffraction image consists of vertical bright lines standing in a direction oblique to the horizontal axis. We will call this direction the image axis. When we rotate the optical grating in the sense that θ increases, the inclination of image axis approaches the horizontal line and the distance D between each two lines becomes larger, and at $\theta = 90°$, D becomes maximum.

The formulae for its apparent grid constant at θ can be obtained by a simple geometrical consideration as shown in Fig. 3.

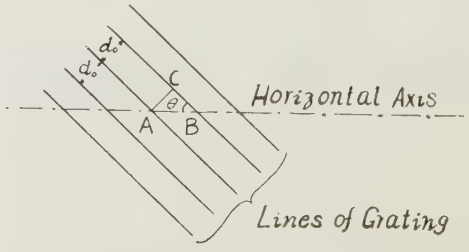

Fig. 3 The consideration for the apparent grid constant

Taking d_0 and d as the original and the apparent grid constant respectively, we

get $AB = AC \operatorname{cosec}\theta$, i. e.

$$d = d_0 \operatorname{cosec}\theta . \qquad (1)$$

In order to verify experimentally the above relation, we photographed the diffration images corresponding to many rotating angles. From the formula for diffraction grating $\sin\varphi = n\lambda/d$, we get $D_n/L = n\lambda/d$, since φ is small in this case. Here $2D_n$ is the distance between two nth order lines of diffraction image on the photographic plate, and L is the effective distance between the grating and the photographic plate. Therefore, we get

$$d = (D_{n0}/D_n)d_0 , \qquad (2)$$

where D_{n0} means the distance D_n when the apparent grid constant d coincides with the original grid constant d_0.

The grating is rotated by means of a mechanism of worm gear and dial. Thirty-five revolutions of the dial rotate the grating by the angle 90°. Therefore one revolution corresponds to 2.571 degrees. Experimental results are shown in Table I, in which $d_0 = 0.2546$ mm which is directly measured by a comparator.

TABLE I. Apparent grid constants of rotatable optical grating

No. of revolution and corresponding degrees	$2D_1$ (mm)	$d = (D_{10}/D_1)d_0$ calculated from the measured value	Theoretical values calculated from $d = d_0 \operatorname{cosec}\theta$
4.5 (11°30′)	1.456	1.360	1.277
7.0 (18°00′)	2.458	0.8060	0.8236
9.5 (24°24′)	3.047	0.6501	0.6161
12.0 (30°54′)	3.886	0.5098	0.4957
14.5 (37°18′)	4.650	0.4260	0.4201
17.0 (43°42′)	5.277	0.3754	0.3685
19.5 (50°48′)	6.005	0.3298	0.3284
24.5 (63°00′)	6.846	0.2893	0.2857
29.5 (76°00′)	7.586	0.2612	0.2623
35.0 (90°00′)	7.781 ($=2D_{10}$)	0.2546	0.2546

Here $2D_1$ is measured by a comparator from the image photographed.

The above data are plotted in Fig. 4. The experimental results and the theoretical values coincide with each other within experimental errors. At the angles smaller than about 12°, the differences between the experimental and theoretical values are comparatively large, but in practice this range of larger error can be avoided by the process which is to be stated in § 5.

4. Procedure of measuring ultrasonic sound velocities

We set a rotatable optical grating perpendicularly to the ultrasonic grating. Then the diffraction image proper to the sample liquid appears as shown in Fig. 5, (A). When we rotate the grating, two lines appear from each original line on its both sides, proceeding in the direction of arrows as shown in Fig. 5, (B), (C) and (D). And when the apparent grid constant of the optical grating coincides with the grid constant of the ultrasonic grating, the image becomes again that as shown in (A).

We have measured by our method the ultrasonic velocities of several liquids.

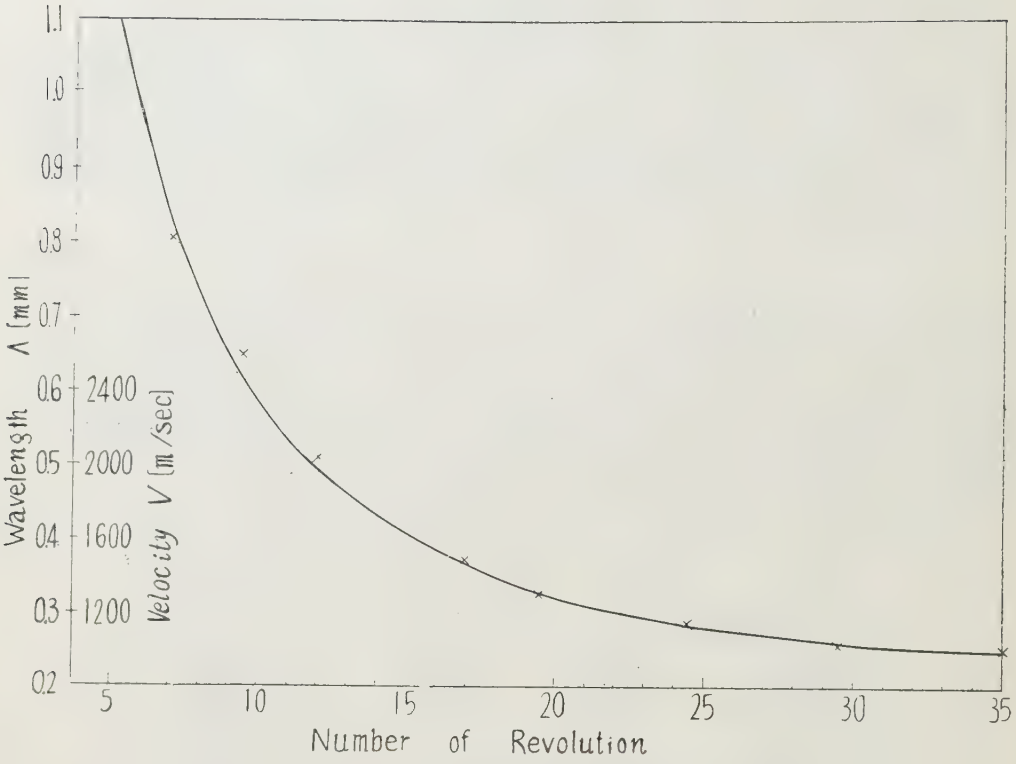

Fig. 4 Relation between wavelength and number of revolution
— Theoretical curve
× Experimental points.

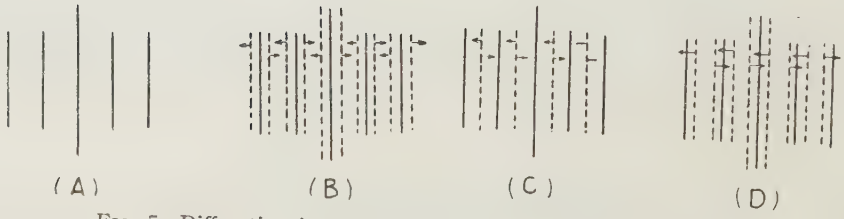

Fig. 5 Diffraction images when the optical grating is rotated.

They are shown in Table II.

TABLE II. Ultrasonic sound velocities measured at frequency 4Mc/s and temperature 30°C.

Liquid	Molecular formulae	No. of Revolution	Column I		Column II		(1) (2) Ref. data
			Λ [mm]	V [m/s]	Λ [mm]	V [m/s]	V [m/s]
Water	H_2O	16.24	0.3822	1529	0.3907	1563	1510
Ethyl-alcohol	C_2H_5OH	21.44	0.3103	1241	0.3142	1257	1134
Amyl-alcohol	$C_5H_{11}OH$	22.42	0.3013	1205	0.3062	1225	
Benzene	C_6H_6	20.73	0.3174	1270	0.3198	1280	1276
Ethyl Benzene	$C_6H_5C_2H_5$	20.25	0.3227	1291	0.3237	1295	
Glycerine	$C_3H_5(OH)_3$	11.54	0.5142	2057	0.5356	2142	1905
Chloric acid	HCl	16.52	0.3771	1508	0.3850	1540	
Ethyl ether	$(C_2H_5)_2O$	>35.00	<0.2546	<1018	<0.2546	<1018	949
Chloroform	$CHCl_3$	>35.00	<0.2546	<1018	<0.2546	<1018	967

The values in column I are calculated according to the law $d = d_0 \operatorname{cosec}\theta$, while those in column II, being added for comparison, are obtained by interpolation using the points which have been determined experimentally and are given in the third column of Table I. The samples other than water were not distilled, so that they might contain some impurities which might cause some deviations from the reference data. We could not obtain the values for ethyl-ether and chloroform, because the value of d_0 of the grating which is available for us at present is not sufficiently small. But if we have an adequate grating, we can easily obtain the values of those samples.

The measuring range of our present apparatus begins from 1020 [m/s], but beyond 2000 [m/s] the experimental error becomes large because of the character of $\operatorname{cosec}\theta$ at smaller θ's. The accuracy of the measurement is 4×10^{-4} at larger angles and 1×10^{-3} at smaller angles.

5. Conclusion

The reliability of this apparatus depends largely upon the rotating mechanism. If it acts satisfactorily, this method is very convenient because the measurement can be performed very speedily. In order to raise the accuracy, it is recommended to divide the measuring range into two parts, namely A (900 m/s~1500 m/s) and B (1400 m/s~2000 m/s) and take adequate values of d_0 for A and B respectively, because we can then avoid the part of $\operatorname{cosec}\theta$ in which this function changes steeply. For example, against the frequency 4Mc/s, the values $d_0 = 0.2240$ mm for A and $d_0 = 0.3500$ mm for B can be selected.

REFERENCES

1. BERGMANN, *Ultrasonics.*
2. P. DEBYE and F. W. SEARS, 'On the Scattering of Light by Supersonic Waves', *Proc. Nat. Acad. Sci.* **18** (1932), 6.
3. A. WEISSLER, 'Ultrasonic Investigation of Molecular Properties of Liquid', *J. Amer. Chem. Soc.* **71** (1949), 419–421.
4. K. SHIBA, *Butsuri Jôsû Hyô* (*Tables of Physical Constants*).

Memoirs of the College of Science, University of Kyoto, Series A,
Vol. XXVII, No. 1, Article 7, 1953

DETERMINATION OF ULTRASONIC SOUND VELOCITIES AND ELASTIC CONSTANTS OF SOLID

BY

Isao TAKAHASHI and Yoshio ISHIDA

(*Received October 29, 1951*)

1. Introduction

We have measured the variation of transmission of ultrasonic sound beam through a solid plate immersed in liquid, when either the thickness of the plate or the incident angle is changed. From the above data, we have determined the velocities of two elastic waves, longitudinal and transversal, in the solid, applying the results developed from the theory of Rayleigh(**1**) and that of Reissner(**2**). From these sound velocities, we have calculated the elastic constants of the solid, using the well-known formulae.

In order to measure the variation of transmission of ultrasonic sound beam, we used the method utilizing the ultrasonic light diffraction phenomena found by Debye and Sears. In the light diffraction generated in the liquid by an ultrasonic sound beam which has passed through the solid plate, the number of the highest order of diffraction which can be observed, is proportional to the intensity of ultrasonic sound at the point passed by light beam. By observing the variation of the number of the highest order, we can determine the incident angles, at which the intensity of ultrasonic sound which has passed through the solid plate, becomes maximum or minimum.

From the experimental results which we have got about aluminium, applying the above method, we have determined the two sound velocities and the elastic constants of aluminium.

2. The results developed from the theory of Rayleigh and that of Reissner

A. The results from the theory of Rayleigh

Rayleigh has studied the velocity potential of the reflected wave, when the longitudinal elastic wave is incident to the plane parallel medium [1] of density ρ_1 and thickness d, from the medium [0] of density ρ. From this result, we get the following formulae:

a) The conditions for transmission to be maximum or minimum in the case of normal incidence are:

$$V\rho = V_L\rho_1\,, \qquad \text{for maximum only,} \tag{1}$$

where V and V_L are longitudinal velocities in both media, and

$$\left.\begin{aligned} d &= m\frac{\lambda_L}{2} \qquad \text{for maximum,} \\ d &= (2m+1)\frac{\lambda_L}{4} \qquad \text{for minimum,} \end{aligned}\right\} \tag{2}$$

where m is 0 or a positive integer, and λ_L is the longitudinal wavelength in the midium [1].

b) The conditions for transmission to be maximum or minimum in the case of oblique incidence are:

$$\left(\frac{\rho_1^2}{\rho^2} - \frac{V^2}{V_L^2}\right)\cot^2\theta_i = \frac{V^2}{V_L^2} - 1 \quad \text{for maximum only,} \quad (3)$$

where θ_i is the intromitting angle as Rayleigh named, at which the whole wave energy can pass through the medium [1], and this angle is independent of the thickness of the medium [1] and

$$\sin^2\theta = \left(\frac{V}{V_L}\right)^2 - \left(\frac{m\lambda}{2}\right)^2\frac{1}{d^2} \qquad \text{for maximum,} \quad (4)$$

and

$$\sin^2\theta = \left(\frac{V}{V_L}\right)^2 - \left(\frac{2m+1}{2}\right)^2\left(\frac{\lambda}{2}\right)^2\frac{1}{d^2} \qquad \text{for minimum.} \quad (4')$$

B. The results from the theory of Reissner

Reissner has calculated the transmission on the assumption that the longitudinal and transversal waves are induced in the solid plate by the longitudinal wave in the surrounding liquid. From this result, we get the following conditions, for the transmission to be maximum,

$$\sin^2\theta = \frac{1}{2}\left(\frac{V}{V_T}\right)^2, \quad (5)$$

$$\sin^2\theta = \left(\frac{V}{V_T}\right)^2 - \left(\frac{m\lambda}{2}\right)^2\frac{1}{d^2}, \quad (6)$$

and

$$\sin^2\theta = \left(\frac{m\lambda}{2}\right)^2\frac{1}{d^2}, \quad (7)$$

where V, λ are respectively the sound velocity and wavelength in the liquid and V_T is the transversal velocity in the solid.

It is interesting that the condition (4) in the case of longitudinal wave has the same form as the condition (6) in the case of transversal wave. In practice, it is difficult to determine the number of order m of the observed maximum corresponding to (4). In Reissner's case, we have, besides (6), the condition (7) which is helpful to determine m. And moreover, we can find the angle θ which satisfies equations (5), (6) and (7) simultaneously and determine the transversal wave velocity V.

3. Experimental procedure

The experimental arrangement is shown in Fig. 1. An ultrasonic sound beam is generated by a quartz crystal in the vessel filled with water. A solid plate can be rotated about the axis perpendicular to the plane of the figure. The number of the highest order of diffraction and the intensity of each spectral line vary with the thickness of the plate and the incident angle.

Relations between the sound intensity at the point passed by light on one hand,

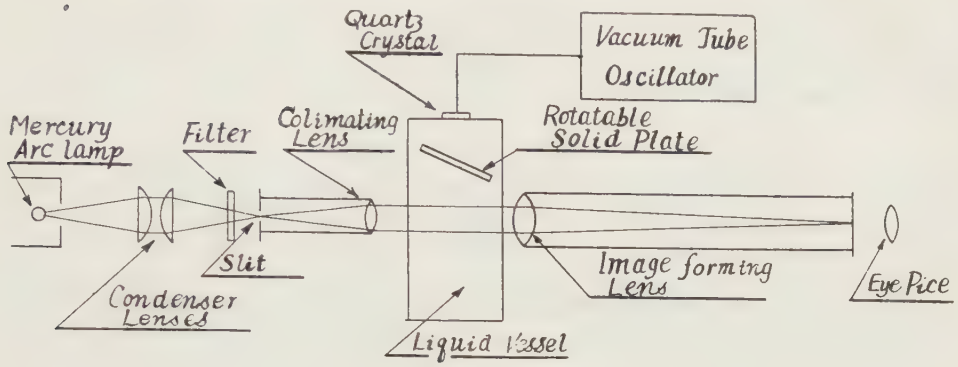

FIG. 1. Experimental arrangement.

and the number of the highest order of diffraction and the intensity of each spectral line on the other, are the following:

1. The stronger the sound intensity is, the higher order appears.
2. The stronger the intensity of the highest order is, the larger is the sound intensity.

According to the above principle, when we observe the transmission intensity of ultrasonic beam, by rotating the solid plate whose thickness is constant, we can find that the intensity of the transmitted beam changes periodically with the angle rotated. The positions of maximum and minimum which appear at that time, can be determined within the error of 0.1°. In the case of aluminium, we get the transmission patterns as shown in Fig. 2. The ordinate of this diagram is the highest order of diffraction which shows the measure of the sound intensity.

A. Determination of longitudinal velocity

We have found the thickness, at which the transmission becomes maximum or minimum for normal incidence, by changing continuously the thickness of the Al-plate by means of roller pressing. From these data, we can determine, using formula (2) the longitudinal velocity V_L, as shown in Table 1.

TABLE 1. Longitudinal wavelength for normal incidence (frequency 3940 Kc, temp. 25.8 ± 1.5°C)

thickness d	$1.92 = \frac{5}{4}\lambda_L$	$1.63 = \lambda_L$	$1.19 = \frac{3}{4}\lambda_L$	$0.85 = \frac{1}{2}\lambda_L$
wavelength λ_L	1.53	1.63	1.59	1.70
mean value of λ_L: $\overline{\lambda_L} = 1.61$ mm				

From $\overline{\lambda_L}$, we get

$$V = \overline{\lambda_L} f = 6350 \pm 350 \text{ [m/sec]}.$$

For oblique incidence, we calculated V_L from the first maximum or minimum in Fig. 2, using formula (4) or (4′). The result is shown in Table 2.

TABLE 2. Longitudinal wavelength for oblique incidence

thickness d	incident angle θ		order m	λ_L [mm]	V_L [m/sec]
1.92	8.4	max.	2	1.54	6070
1.63	10.2	min.	1	1.53	6030
1.19	10.3	max.	1	1.58	6230
0.85	9.4	min.	0	1.93	7550

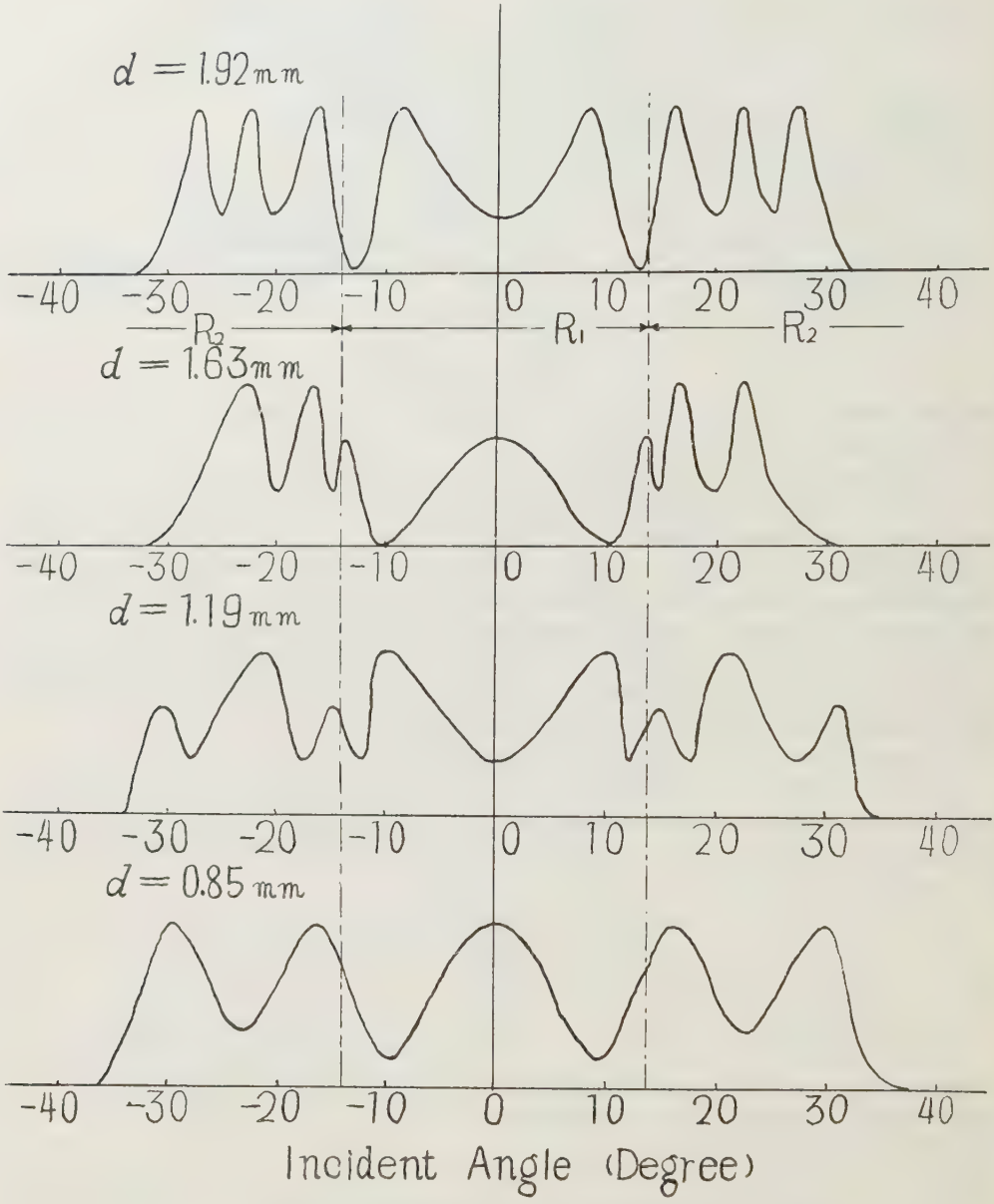

FIG. 2. Transmission patterns of aluminium.

The values of λ_L and V_L in the first three rows show rough coincidence, but the values in the last row is considerably apart from others.

We have calculated the total reflection angle $\theta_C = 13.4°$, according to $\sin\theta_C = V/V_L$, using the values $V_L = 6350$ [m/sec] and $V = 1500$ [m/sec]. This angle is shown by broken line in Fig. 2. We get two regions R_1 and R_2 on one side separated by this line. And in R_2, longitudinal wave and transversal one coexist, but in R_2 only transversal wave exists. We have expected that the transmission minimum will appear at the angle

θc for any thickness, because this angle is independent of the thickness. But in our experiment about aluminium, the transmission minimum has not appeared at this angle. From this fact, we have deduced that in region R_1 the transversal wave is co-existing.

B. Detemination of transversal velocity

The determination of the transversal velocity can be performed by finding such θ which satisfies (5), (6) and (7), by using maximum points in R_2. Applying formulae (5), (6) and (7) to these points summarized in Table 3, we determine the transversal velocity diagrammatically. If we take $\sin^2\theta$ as ordinate, $1/d^2$ as abscissa and m as parameter in Fig. 3, the formula (6) corresponds to a group of straight lines passing through a common point on the ordinate axis, and the formula (7) to a group of straight lines passing through the origin.

We plot on this graph the measured points shown in Table 3, and, selecting adequate several points, we draw such straight lines as pass through a common point on the ordinate axis, which are called $(a_1, a_2, \cdots, a_6)$, corresponding to $m=1, 2, \cdots 6$ and as the whole group (a). Straight lines of group (a) satisfy the formula (6). Next, λ in formula (7) can be computed to 0.381 mm, from the sound velocity in water and the frequency. Giving m integral values $(1, 2, \cdots 6)$ successively in (7), we get a group of straight lines $b\,(b_1, b_2, \cdots b_6)$, corresponding to $m=1, 2, \cdots, 6$, which satisfies formula (7). In the third place, we must find the angle θ independent of the thickness. As easily seen from the forms of the formulae (5), (6) and (7), such θ ought to be on the intersections $(P_1, P_2, \cdots P_6)$ of two straight lines of (a) and (b) with the same suffix. In practice, we get $\sin^2\theta = 0.169$ as the mean value of ordinates of these points. We

TABLE 3. Maximum points in region R_2

d [mm]	θ	$\sin\theta$	$\sin^2\theta$	$1/d^2$
3.016	16.1	0.2773	0.077	0.11
3.016	19.3	0.3305	0.109	0.11
3.016	23.0	0.3907	0.152	0.11
3.016	25.5	0.4305	0.185	0.11
1.92	16.1	0.2773	0.077	0.271
1.92	22.0	0.3746	0.140	0.271
1.92	26.9	0.4524	0.204	0.271
1.63	13.6	0.2351	0.055	0.377
1.63	16.3	0.2807	0.079	0.377
1.63	22.0	0.3746	0.140	0.377
1.19	14.6	0.2521	0.063	0.708
1.19	20.9	0.3567	0.127	0.708
1.19	30.4	0.5060	0.256	0.708
1.035	18.0	0.3090	0.095	0.935
1.035	23.4	0.3971	0.157	0.935
1.035	30.2	0.5030	0.252	0.935
0.85	16.0	0.2756	0.076	1.39
0.85	29.2	0.4879	0.237	1.39
0.72	14.0	0.2419	0.058	1.94
0.72	28.8	0.4818	0.230	1.94

use this value and the sound velocity in water $V=1500$ [m/sec] in formula (5). We get

$$V = 2580 \pm 140 \text{ [m/sec]}$$

as the transversal velocity.

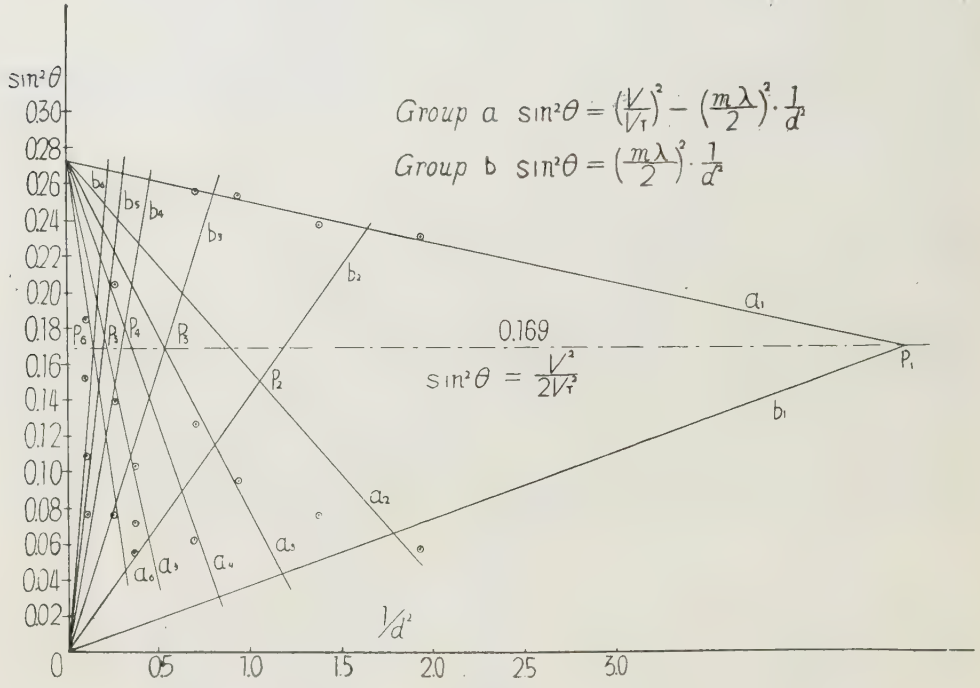

FIG. 3. Diagrammatical determination of transversal velocity.

4. Calculation of elastic constants

In order to calculate the elastic constants, we use following formulae:

$$V_L = \sqrt{\frac{\lambda + 2\mu}{\rho}}, \tag{8}$$

$$V_T = \sqrt{\frac{\mu}{\rho}}, \tag{9}$$

$$E = \frac{\mu(3\lambda + 2\mu)}{\lambda + \mu}, \tag{10}$$

and

$$\sigma = \frac{\lambda}{2(\lambda + \mu)}, \tag{11}$$

where λ and μ are Lamé constants, E Young's modulus and σ Poisson's ratio.

Our results, together with those obtained by other writers, are summarized in Table 4.

TABLE 4. Elastic constants of aluminium

V_L [m/sec]	V_T [m/sec]	$E \times 10^{-11}$ [dyne/cm^2]	$\mu \times 10^{-11}$ [dyne/cm^2]	σ	experimenter
6350 ± 350	2580 ± 140	5.00	1.78	0.400	Present authors
7050	2820	6.45	2.14	0.400	W. C. Schneider & C. J. Burton
5104					Masson (Handbook)

It will be seen that there is a great difference between the value of V_L found by Schneider and Burton (3) and the corresponding value obtained by Masson and that our value lies between these two.

REFERENCES

1. LORD RAYLEIGH, Theory of Sound, Vol. 2, 86.
2. H. REISSNER, *Helv. Phys. Acta*, **11** (1938), 140.
3. W. C. SCHNEIDER & C. J. BURTON: *J. Appl. Phys.*, **20** (1949), 48.

Memoirs of the College of Science, University of Kyoto, Series A,
Vol. XXVII, No. 1, Article 8, 1953

MICROCLIMATIC STUDY, II
A NEW TYPE THERMOJUNCTION FOR MICROCLIMATIC USE

BY

Ken-ichi TAKASU

(*Received January 28, 1952*)

1. Introduction

Upon microclimatic temperature measurement a radiation shield is of general use to be free from radiation error, the use of such, however, may affect the microclimatic state under observation to deviate from the natural state. It would not be without any effect upon temperature of a few millimetres air layer, even if an extremely small type shield should be employed to restrict the shade as small as possible. As it is well known, the controlling factors of the microclimatic state are the thermal economy at the earth's surface and the degree of turbulence in the adjacent air layer, these two factors must not be affected by measurement itself. Accordingly, only the smallest number of apparatus should be set up near the measuring portion. Thus a method of removal of radiation error without using shield in the measuring portion is considered in the following discussion.

2. A compensated thermojunction

In addition to the measuring element J_1 and cold element J_2, as indicated in the diagram, another compensating elements named J_3 and J_4 are employed. All the elements except J_1 are set at a distance from the measuring portion so that the general microclimatic state should remain undisturbed. All the elements are constructed in the same form and the compensating elements should be placed very close to each other, J_4, one of them, having small shine cover. Then J_3 and J_4 are in the same temperature and only J_3 receives the solar radiation, and the E. M. F. between J_3 and J_4 is due to the rise of temperature by solar radiation. This compensates the E. M. F. introduced by similar solar radiation between J_1 and J_2, showing now only the air temperature of the measuring portion, that is $J_2 - J_1 - J_3 - J_4$.

3. A testing example

A testing example on the short cripped lawn is shown on Plate I, which is the measurement of air temperature at the layer almost touching the ground. In the Plate, (a) is the record by the new type compensated junction and (b) the record by usual thermojunction without radiation shield, (c) the record of E. M. F. on a pair of same shaped thermocouples, placed closely to each other and only one of them screened, that is $J_3 - J_4$.

These are simultaneous records and the wind velocity by hot-wire anemometer and solar energy by Gorczinsky's solarimeter are added as references.

On this record, it is clearly shown that the uncompensated and exposed junction (b) received direct effect of solar radiation. This fact becomes more evident when

mean state is considered and the compensated junction shows true temperature even the measuring element exposed to sunshine.

TABLE 1.

		14^h25^m—36^m	52^m—55^m
(a)	$J_2-J_1-J_3-J_4$	22.98°	22.51°
(b)	J_2-J_1	27.81	26.68
(b)—(a)	(calculated)	4.83	4.17
(c)	J_3-J_4 (measured)	4.96	4.02

(showing mean values of every 10 readings respectively)

In these tests the writer used the relatively thick wires (0.25mm) to get the larger radiation effect. Usually thin wires less than 0.2mm in diameter are used and the error should be smaller than these values.

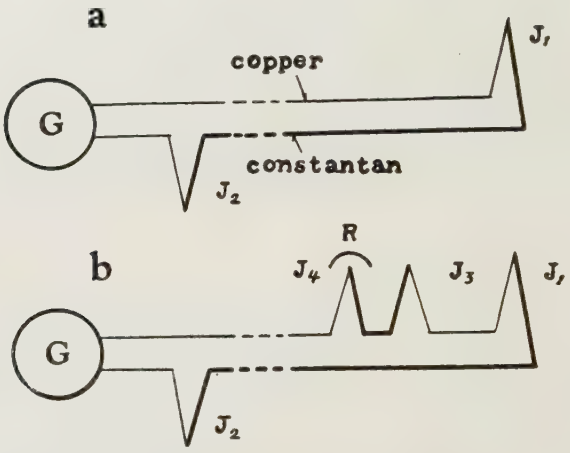

FIG. 1. Diagram of the thermojunction

a) Usual type

b) New type

J_1 ..... Measuring element

J_2 ..... Cold (constant) element

J_3, J_4 ..... Compensating element

R ..... Radiation shield

G ..... Galvanometer

4. Remarks

It is evident that all the possible radiation including direct sunshine must be avoided to get the true temperature, and this may be accomplished in similar manner. However, it may be enough for the present purpose if the largest radiation, i. e., direct solar radiation, is successfully removed. Applying this method, the temperature of leaf surface or skin-temperature of human body under the direct sunshine can be measured without disturbing the natural state.

PLATE I

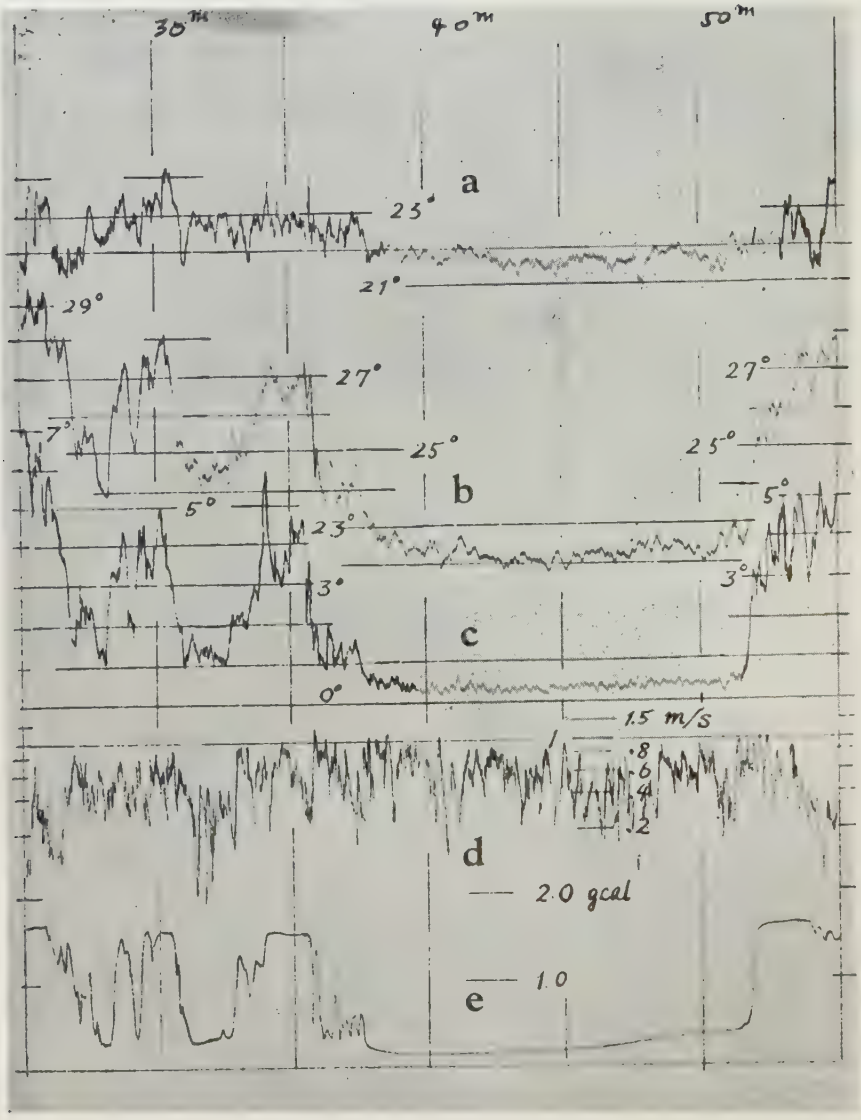

A testing example of the thermojunctions on the lawn of Met. Res. Inst., Kyoto Univ. at 14^h25–55^m, 13 April, 1950. (Weather: calm, 3/10 Cu)

a) Air temperature measured by the compensated thermojunction.
b) Air temperature measured by the usual type thermojunction without radiation shield.
c) The record of E. M. F. on the pair of same shaped thermocouples, one of them having been screened.
d) Wind velocity measured by hot-wire anemometer.
e) Solar radiation measured by Gorczynsky's solarimeter.

Memoirs of the College of Science, University of Kyoto, Series A,
Vol. XXVII, No. 1, Article 9, 1953

MICROCLIMATIC STUDY, III
A WORKING METHOD FOR FINDING AUSTAUSCH COEFFICIENTS FROM THE RECORDS OF TEMPERATURE FLUCTUATIONS

BY

Ken-ichi TAKASU

(*Received January 28, 1952*)

1. Introduction

In spite of tremendous development achieved in the realm of atmospheric turbulence, the modern meteorology has so far been prevented from further development by lack of quantitative studies on the Austausch coefficient. Especially in the field of the micrometeorology concerning the lowest layer of the atmosphere, deficiency in the data has been preventing successful solution of many vital problems. Since Sverdrup (**1**) has started to solve the similar problem on the snow field, several reports have been published, but remarkable disagreement was seen in the values of the Austausch coefficient.

As is well known, the methods of finding the Austausch coefficient can be divided into the following two ways : the indirect method, in which the Austausch coefficient is calculated from the variation and distribution of mean state using the equation of eddy transfer, and the direct method, which deals with derivation from the mean state owing to the turbulent mixing. The latter seems to be better for calculating the Austausch coefficient during a certain period of time at a certain place. It seems quite natural to the present writer (**2**) who devised a new type self-recorder and obtained the records of small turbulent oscillation, to attempt to calculate the Austausch coefficient from these records. The writer originally wished to apply Ertel's method (**3**) which had looked most suitable for our purpose, but gave up the scheme, since some doubt arose in the principle of the method, and therefore decided to make a working method suitable for calculation of the coefficient from the records he had obtained, by improving the older method.

2. Discussion on Hesselberg's method

The principle of Hesselberg's method (**4**) is as follows :—

(i) The oscillating period of turbulence is at random, but there exists the mean period P which is almost constant. This P is significant.

(ii) The mixing length l can take any value between 0 and $\frac{1}{2}Pw$, but for convenience the mean value $\frac{1}{4}Pw$ is adopted for l, where w is the vertical component of the eddy velocity, namely :

$$l = -\frac{1}{4}Pw\,. \qquad (1)$$

(iii) Then the Austausch coefficient $A = -\rho\overline{wl}$, where ρ is the density of the air, becomes

$$A = \frac{1}{4} P \rho \overline{w^2}, \tag{2}$$

and when w obeys Maxwell's distribution law we have

$$A = \frac{1}{8} P \rho k, \tag{3}$$

where k is a certain unknown constant.

In order to use equation (2), it is necessary to know about $\overline{w^2}$. It is well known, however, that measurement of w is extremely difficult. While, equation (3) does not give directly the numerical value of the Austausch coefficient A because of the unknown constant k.

Although we may lay aside the fact that the assumption (1) for the mixing length l seems to be somewhat too bald, yet Hesselberg's method still suffers from a drawback that it is extremely difficult to obtain the mean period P in random fluctuation and in practice considerable personal error in obtaining it cannot be avoided.

3. Discussion on Ertel's method

The principle of Ertel's method (3) is as follows :—

(i) Let s be a fluctuating element, $\bar{s}$ its time-mean, l the mixing length and z the height. Then, we have

$$s = \bar{s} + l \frac{\partial \bar{s}}{\partial z}, \tag{4}$$

which gives

$$l = \frac{s - \bar{s}}{\partial \bar{s} / \partial z}.$$

Thus, the mixing length l can be calculated by using the values of $s - \bar{s}$ and $\partial \bar{s}/\partial z$ as obtained from the observed records.

(ii) As to the relationship between l and w, Ertel adopted Prandtl's assumptions $l \propto u$, $u \propto w$ and assumed that

$$l = - cw, \tag{5}$$

where c is a certain unknown constant.

(iii) Then the Austausch coefficient $A = - \rho \overline{wl}$ becomes

$$A = c \rho \overline{w^2} = \frac{\rho \overline{(s - \bar{s})^2}}{c (\partial \bar{s} / \partial z)^2}. \tag{6}$$

(iv) For the unknown constant c in this equation Hesselberg made use of the value $\frac{1}{4}P$, but Ertel attempted to eliminate it by assuming that s should be conserved. Then we have

$$\frac{ds}{dt} = 0. \tag{7}$$

Since, however, $\partial \bar{s}/\partial t = 0$, it follows from (7) that

$$-\frac{\partial s}{\partial t} = w\frac{\partial \bar{s}}{\partial z}, \qquad (8)$$

which gives

$$w = \overline{\left|\frac{\partial s}{\partial t}\right|} \Big/ \frac{\partial \bar{s}}{\partial z}. \qquad (9)$$

On the other hand, we have, from (4) and (5),

$$\bar{w} = \frac{\overline{|l|}}{c} = \frac{\overline{|s - \bar{s}|}}{c(\partial \bar{s}/\partial z)}. \qquad (10)$$

If we assume that the turbulent velocity w obeys Gauss's distribution law, the following Cornu's relation may be used:

$$2\overline{w^2} = \pi\overline{|w^2|}. \qquad (11)$$

Thus, the Austausch coefficient A becomes ultimately

$$A = \rho c\overline{w^2} = \rho c\frac{\pi}{2}\overline{|w|^2} = \rho\frac{\pi}{2}\frac{\overline{|s - \bar{s}|}\,\overline{|\partial s/\partial t|}}{(\partial \bar{s}/\partial z)^2}. \qquad (12)$$

Ertel (3) has further made a refinement and has given the following expression for the Austausch coefficient. Thus,

$$A = \rho\frac{S_m(s)\,S_m(\partial s/\partial t)}{(\partial \bar{s}/\partial z)^2}, \qquad (13)$$

where S_m means the mean deviation in the sense of the theory of errors. In practice, $S_m(s)$ and $S_m(\partial s\ \partial t)$ can be obtained as follows by using observed values $s_i\,(i = 1, 2, \cdots, n)$ taken at equal time-interval Δt from the records:

$$S_m(s) = \sqrt{\frac{\sum(s - \bar{s})^2}{n}},$$

$$S_m(\partial s/\partial t) = \frac{1}{\Delta t}\sqrt{\frac{\sum_{i=1}^{n-1}(s_{i+1} - s_i)^2}{n - 1}}.$$

The above formula (13) can be applied in practice to calculating the Austausch coefficient by using acutual observed records, and indeed Lettau (5) tried to apply the formula, but no adequate records could be found.

The above Ertel's method is characteristic in that the unknown constant c is eliminated by introducing the value of $\partial s/\partial t$, but this very point is not entirely free from question.

Eq. (7) or eq. (8) conveys the same idea as eq. (4), and both are based upon the assumption of the conservation of the fluctuating physical element which is transported by moving eddies. But, differentiation of (4) with respect to the time gives

$$\frac{\partial s}{\partial t} = \frac{\partial l}{\partial t}\frac{\partial \bar{s}}{\partial z},$$

which is not in accord with (8), since $\partial l/\partial t = w$.

As an another example, let us consider a simple model such as $s=\bar{s}+a\sin\sigma t$. In this case, l is found to be proportional to $\sin\sigma t$, and since $\partial s/\partial t=-a\sigma\cos\sigma t$, w is proportional to $\cos\sigma t$. Thus, the relation (5) between l and w can no longer be always satisfied independently of the time. In other words, the two relations (4) and (8) contradict to each other, proving failure of Ertel's method.

4. A working method proposed by the present author

Following the priciple mentioned above and combining Ertel's intermediate formula (6), namely:

$$A=\frac{\rho\overline{(s-\bar{s})^2}}{c\overline{(\partial\bar{s}/\partial z)^2}}$$

with Hesselberg's relation $c=\frac{1}{4}P$, the present author now proposes a working formula of the form:

$$A=\frac{4\rho\overline{(s-\bar{s})^2}}{P\overline{(\partial\bar{s}/\partial z)^2}}. \tag{14}$$

Then the coefficient of eddy transfer can be calculated by using our observed records:

(i) Acutually, the fluctuating curves appeared on the records are the result of superposition of the oscillations with various periods and amplitudes, and the shorter the period, the larger the mechanical decaying factor of the amplitude, so that the variation with extremely short period disappears from our records. Hence we must examine the influence of the existence of such an extremely short periodic oscillation upon the Austausch coefficient.

If we assume that $s-\bar{s}=a\sin\sigma t$ with $\sigma=2\pi/P$, we have, from (14),

$$A=\frac{4\rho}{P}\frac{a^2P^{-1}\int_0^P\sin^2\sigma t\,dt}{\overline{(\partial\bar{s}/\partial z)^2}}=\frac{2a^2\rho}{P}\frac{1}{\overline{(\partial\bar{s}/\partial z)^2}},$$

or

$$A=\frac{R^2\rho}{2P}\frac{1}{\overline{(\partial\bar{s}/\partial z)^2}}, \tag{15}$$

where $R\,(=2a)$ is the range of the oscillation.

Thus, it is found that the Austausch coefficient A is proportional to R^2/P, so that if $R_1^2/P_1\ll R_2^2/P_2$ the coefficient A is not affected by the existence of the oscillation with R_1^2/P_1.

(ii) The time scale of our recorder is of about 1 millimetres per 10 seconds, so that the mean value and range over 20 seconds were calculated.

(a) Let s be the mean value over 20 seconds and also let $\bar{s}$ be the mean value of s over 10 minutes. Using these values we calculate the value of A_l as defined by

$$K_l=\frac{A_l}{\rho}=\frac{4\overline{(s-\bar{s})^2}}{P\overline{(\partial\bar{s}/\partial z)^2}}. \tag{16}$$

This formula can legitimately be used, since there are more than thirty values of $s-\bar{s}$ taken from the records. If n is the number of maximum or minimum points of the variation curve of $s-\bar{s}$, the mean period P is given by $(10\times60)/n$ sec, although not

always clear-cut as desired.

(b) Our recorder is not fast enough to be capable of reading several points within 20 seconds, and a more rapidly rolling recorder must be employed. Thus, we are obliged to assume $s-\bar{s}=R\sin(2\pi t/P)$ with $P=20$ sec for the variations within 20 seconds, where R is the mean value over 10 minutes of the ranges (i. e. maximum minus minimum) in 20 seconds interval. Then we calculate the value of A_s as defined by

$$K_s=\frac{A_s}{\rho}=\frac{1}{40}\frac{R^2}{(\partial\bar{s}/\partial z)^2}. \tag{17}$$

(iii) If $A_t \gg A_s$, then A_t may be regarded as the Austausch coefficient. But, if $A_t \fallingdotseq A_s$ or $A_t < A_s$, some difficulties arise. Since the Austausch coefficient A is believed to depend upon the time scale, the difference between A_t and A_s may be caused by the scale differences. Further discussion on this point will be made in due time.

(iv) In applying the author's working method of calculating the Austausch coefficient, it is necessary to know the value of $\partial\bar{s}/\partial z$. It often occurs that the value of A depends more upon $(\partial\bar{s}/\partial z)^2$ than upon $\overline{(s-\bar{s})^2}$, so that the more precise value of $\partial\bar{s}/\partial z$ is requested. In order to obtain such a precise value of $\partial\bar{s}/\partial z$, it is desirable to make use of the junctions made specially for this purpose. Since, however, the number of junctions is limited in the actual observations, such a value may be obtained, in most cases, graphically from the values of temperatures at several heights. Therefore, considerable personal error cannot be avoided. It is to be noted here that the above method of calculating the value of A is by no means applicable to all cases, since it is not seldom that the value of $\partial\bar{s}/\partial z$ cannot be obtained directly.

5. An indirect method of calculating A from the mean state

As an addendum, an indirect method of calculating the Austausch coefficient A from the mean state is given. Let us assume that the following relation holds good:

$$\frac{\partial\bar{s}}{\partial t}=\frac{\partial}{\partial z}\left(K\frac{\partial\bar{s}}{\partial z}\right), \qquad (K=A\rho).$$

(When $\bar{s}$ represents the temperature, this relation does not always hold good in case when the radiation effects as well as other effects are taken into account.) Also we take for $\partial\bar{s}/\partial t$ the value of $\Delta s/\Delta t$ in 5 or 10 minutes. We estimate the values of $\partial^2\bar{s}/\partial z^2$ and $\partial\bar{s}/\partial z$ graphically from the vertical distribution curve of $\bar{s}$.

Let a first approximation of K be K_1 which is given by

$$K_1=\frac{\partial\bar{s}}{\partial t}\Big/\frac{\partial^2\bar{s}}{\partial z^2}.$$

Then, making use of the value of $\partial K_1/\partial z$ as obtained by plotting the value of K_1 against height, the value of K can be calculated approximately by the following equation:

$$K=\left(\frac{\partial\bar{s}}{\partial t}-\frac{\partial K_1}{\partial z}\frac{\partial\bar{s}}{\partial z}\right)\Big/\frac{\partial^2\bar{s}}{\partial z^2}.$$

6. An example

(i) Data: The survey over the frozen lake of Suwa, from 15^h05^m to 10^m on Feb. 1,

1943. The original record is given on Plate I.

(ii) The variation of 20 sec mean temperatures and the vertical distribution of mean temperature are shown in Fig. 1.

(iii) The results of observation for 10 minutes from 15^h05^m to 15^m are shown in Table 1.

Table 1.

Height	θ (°C)	R (°C)	$\frac{\partial\theta}{\partial z}$	$\overline{(s-\bar{s})^2}$	K_l	K_s
500 cm	−0.91	0.25	2.8×10^{-3}	0.074	630	199
100	−2.25	0.20	4.1 〃	0.066	262	59.5
50	−2.48	0.27	5.2 〃	0.098	242	67.4
20	−2.68	0.25	9.0 〃	0.066	54.3	19.3
5	−3.07	0.20	26.0 〃	0.035	3.42	1.48

(iv) The results for 5 minutes as obtained by applying the indirect method are shown in Table 2 below.

Table 2.

Height	mean temp. 5^m—10^m	mean temp. 10^m—15^m	$\Delta\theta$	$\frac{\Delta\theta}{\Delta t}$
500 cm	−1.09°	−0.73°	0.36°	1.2×10^{-3}
100	−2.38	−2.11	0.27	0.9 〃
50	−2.62	−2.35	0.27	0.9 〃
20	−2.80	−2.57	0.23	0.77 〃
5	−3.09	−3.04	0.05	0.17 〃

Height	$\frac{\Delta\theta}{\Delta z}$ 5^m—10^m	$\frac{\Delta\theta}{\Delta z}$ 10^m—15^m	$\frac{\Delta^2\theta}{\Delta^2 z}$ 5^m—10^m	$\frac{\Delta^2\theta}{\Delta^2 z}$ 10^m—15^m
500 cm	2.12×10^{-3}	2.54×10^{-3}	4.2×10^{-6}	3.2×10^{-6}
100	4.4 〃	4.1 〃	1.3×10^{-5}	0.9×10^{-5}
50	5.4 〃	5.6 〃	4.0×10^{-5}	7.4×10^{-5}
20	9.0 〃	11.0 〃	2.1×10^{-4}	4.3×10^{-4}
5	28.0 〃	42.0 〃	1.0×10^{-3}	1.8×10^{-3}

Height	$K_1=\frac{\partial\theta}{\partial t}\frac{\partial^2\theta}{\partial z^2}$ 5^m—10^m	$K_1=\frac{\partial\theta}{\partial t}\frac{\partial^2\theta}{\partial z^2}$ 10^m—15^m	$K=\frac{\frac{\partial\theta}{\partial t}-\frac{\partial K_1}{\partial z}\frac{\partial\theta}{\partial z}}{\frac{\partial^2\theta}{\partial^2 z}}$ 5^m—10^m	$K=\frac{\frac{\partial\theta}{\partial t}-\frac{\partial K_1}{\partial z}\frac{\partial\theta}{\partial z}}{\frac{\partial^2\theta}{\partial^2 z}}$ 10^m—15^m
500 cm	285	375	40.5	78.2
100	69.1	100	192	406
50	22.5	12.2	81.0	13.1
20	3.65	1.78	7.23	2.81
5	0.17	0.09	0.95	1.7

REFERENCES

1. H. L. Sverdrup, 'The eddy conductivity of the air over a smooth snowfield.' *Geofisiske Publ.*, **11** (1936), 7.
2. K. Takasu, 'Microclimatic study. I. A new type self-recorder.' *Mem. Coll. Sci. Univ. of Kyoto*, A **25** (1949), 69.
3. H. Ertel, 'Eine Methode zur Berechnung des Austauschkoeffizienten aus den Feinregistrierungen der turbulenten Schwankungen.' *Gerlands Beitr.*, **25** (1930), 279.
4. T. Hesselberg, 'Ein neuer Ausdruck für den Austauschkoeffizienten.' *Ann. Hydr.*, **57** (1929), 319.
5. H. Lettau, *Atmosphärische Turbulenz* (1936), 226.

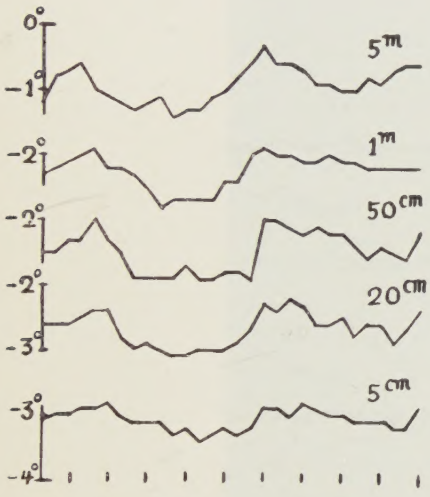

Mean period $P = \frac{600}{10} = 60$ sec.

(a)

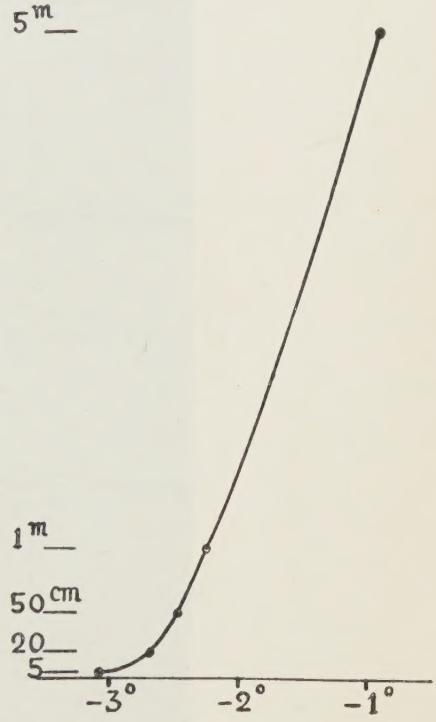

(b)

FIG. 1. a) Variation of 20 sec. mean temperature,
b) Vertical distribution of mean temperature.

PLATE I

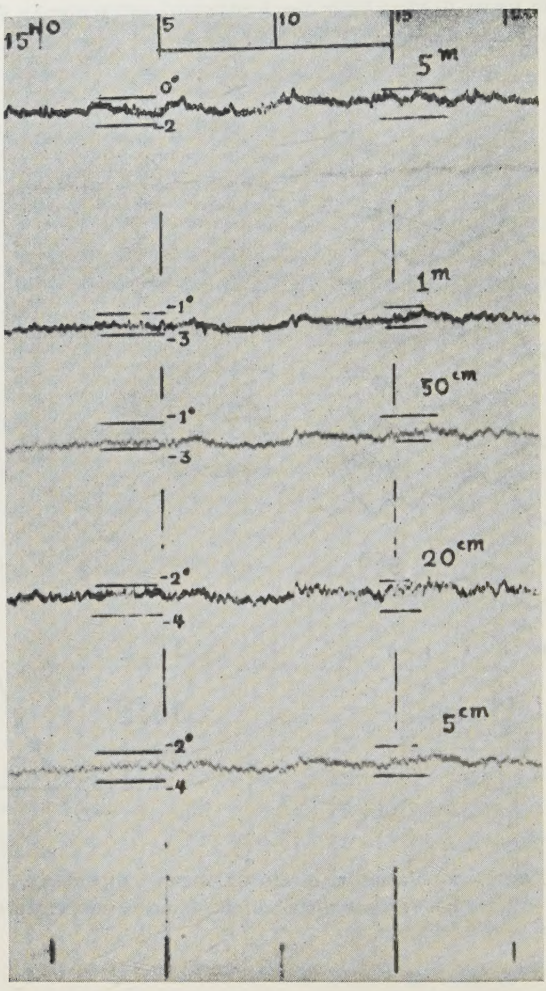

The record of temperatures over the frozen lake of Suwa.
at $15^h\,05^m$–10^m, Feb. 1 1943.
(Weather : Clear and calm)

CONTENTS

A Note on the Skin Friction of a Flat Plate to Oseen's Approximation

BY *S. Tomotika* 1

The Drag on an Elliptic Cylinder moving in a Viscous Liquid at Small Reynolds Numbers

BY *S. Tomotika* AND *H. Yoshinobu* 11

On the Glide Twining in Single Crystals of Tin

BY *Hiroshi Kiho* AND *Ken-ichiro Ishii* 23

On a New Method of Measuring Specific Heat of Metals

BY *Shigeka Nishioka* 31

Effects of Cold Working on Specific Heat of Metals

BY *Shigeka Nishioka* 35

A New Method of Measuring Ultrasonic Sound Velocities in Liquids

BY *Isao Takahashi, Yoshio Ishida* AND *Mitsuo Ôta* 41

Determination of Ultrasonic Sound Velocities and Elastic Constants of Solid

BY *Isao Takahashi* AND *Yoshio Ishida* 47

Microclimatic Study II, A New Type Thermojunction for Microclimatic Use

BY *Ken-Ichi Takasu* 55

Microclimatic Study III, A Working Method For Finding Austausch Coefficients from the Records of Temperature Fluctuations

BY *Ken-Ichi Takasu* 59